Structural basis for phosphatase regulation by the anchoring protein AKAP79

Patrick J. Nygren

A dissertation

submitted in partial fulfillment of the

requirement for the degree of

Doctor of Philosophy

University of Washington

2015

Reading Committee:

John Scott, Chair

Stan McKnight

Rich Gardner

Program authorized to offer degree:

Pharmacology

© Copyright 2015

Patrick J. Nygren

University of Washington

Abstract

Structural basis for phosphatase regulation by the anchoring protein AKAP79

Patrick J. Nygren

Chair of the Supervisory Committee:

Professor John D. Scott

Department of Pharmacology

The calcium/calmodulin-activated protein phosphatase 2B (PP2B, or calcineurin) regulates diverse biological processes including glucose homeostasis and synaptic plasticity. PP2B is targeted to specific substrates, such as the GluRI subunit of the AMPA receptor, by the scaffolding molecule A-kinase anchoring protein 79 (AKAP79), which also interacts with protein kinase A (PKA). AKAP79 contains a short linear motif that is the primary site of interaction with PP2B. We have identified an auxiliary interaction site for PP2B at the N-terminal region of AKAP79. Using hybrid approaches including single particle EM, chemical crosslinking/mass spectrometry, biophysical techniques, and *in vitro* protein-protein interaction assays, I show that this additional interaction exclusively binds activated PP2B through a conserved LxVP mechanism. I mapped a 16 amino acid region in AKAP79 that is necessary for the LxVP interaction and show that the peptide can effectively compete for binding. I use FRET reporters for PP2B activity to show that this auxiliary interaction is important for tuning the activity of PP2B towards specific substrates. Preliminary negative stain EM studies reveal that AKAP79 forms multiple simultaneous contacts with PP2B in the presence of calcium and calmodulin. This structural model shows that AKAP79 has a greater role in regulating PP2B activity and targeting than previously appreciated. This work describes a dynamic model of PP2B anchoring in which the active

phosphatase is anchored differently than the inactive form. A bipartite interaction allows control of localization through the PxIxIT motif, while simultaneously allowing fine control of PP2B sensitivity to calcium through the dynamic LxVP motif.

Table of Contents

List of Figures

Table of Abbreviations

Abbreviation	Full name
AKAP	A-kinase anchoring protein
AMPA	α-amino-3-hydroxy-5-methylisooxazole-4-propionic acid
CaM	calmodulin
CaMKII	Ca2+ /calmodulin-dependent protein kinase II
cAMP	Cyclic adenosine mono phosphate
CaNAR	Calcineurin activity reporter
Cav1.2	Voltage-gated calcium channel 1.2
Cryo-EM	Cryo-electron microscopy
DARPP32	Dopamine- and cAMP-regulated phosphoprotein, Mr 32 kDa
D/D domain	Docking/dimerization domain
diFMUP	6,8-difluoro-4-methylumbelliferyl phosphate
EDTA	Ethylenediaminetetraacetic acid
FK506	Tacrolimus
FKBP	FK506-binding protein
FMP-API-1	3,3'-diamino-4,4'-dihydroxydiphenylmethane
FRET	Förster resonance energy transfer
GluA1	Glutamate AMPA receptor subunit 1
GPCR	G-protein coupled receptor
GST	Glutathione s-transferase
Ht31	Human thyroid clone 31
IPTG	Isopropyl β-D-1-thiogalactopyranoside
MAGUK	Membrane-associated guanylate kinase
mAKAP	Muscle-specific AKAP
MAP2	Microtubule-associated protein 1
MBBR	Membrane binding basic region
MBP	Maltose binding protein
NFAT	Nuclear factor activator of T cells
NMDA	N-methyl D-aspartate
NMR	Nuclear magnetic resonance
PDE	Phosphodiesterase
PIP2	Phosphoinositol 2-phosphate
PKA	Protein kinase A
PKC	Protein kinase C
pNPP	para-Nitrophenylphosphate
PNUTS	PP1 nuclear targeting subunit

PP1	Protein phosphatase 1
PP2B	Protein phosphatase 2B
PSD-95	Postsynaptic density protein 95
RI	PKA regulatory subunit isoform I
RII	PKA regulatory subunit isoform II
RCaMP	Red genetically encoded calcium indicator
RCT	Random conical tilt
SAP97	Synapse associated protein 97
SDS-PAGE	Sodium dodecyl sulfate polyacrylamide gel electrophoresis
SEC-MALS	Size-exclusion chromatography-multiangle light scattering
SLiM	Short linear motif
superAKAPis	Super AKAP *in silico*
XL-MS	Crosslinking-mass spectrometry

Acknowledgments

First I want to thank John Scott, for guiding and mentoring me through this project. John, without your investment in my development as a scientist, my thesis would have been a shadow of itself. I am grateful for the opportunity to work in your group and learn from you. In addition, I am indebted to Lorene for her help with formatting and thinking through how to best layout figures and organize my manuscripts. Mel has been invaluable in keeping our lab group coordinated and on top of administrative details.

I would also like to thank my graduate committee for their guidance and support through this multi-faceted project, and in particular my reading committee, John, Stan, and Rich, for taking time to review this thesis.

My fellow lab members, past and present, have been the best day-to-day support I could ask for. Senior members such as Donelson, Matt, Dave, Simon, Heidi, Emily, Catherine, and Chris offered valuable input and advice almost daily, whilst also being available to commiserate over a beer when their advice went awry. Junior members such as Laura, Rigney, Paula, and Leah, shared their infectious youthful optimism, and also commiserated over beers.

However, the most special friendships were shared with Bret and Jen, who were with me for nearly all of my graduate career, and supported me in personal and professional times through the hardest and the best situations alike, always making sure I had my head on straight. And also commiserated over beers.

In addition, I have had the tremendous privilege of being surrounded by numerous friends in Seattle, who've helped me relax and enjoy this time in my life. I have decompressed and expressed my creativity by being in a band with Max, Cody, and Stephen. I've dreamed about the future over beers and video games with Mario. I've stayed active by climbing with Jessie, Cory, Allison,

Hanna, David, Jacob, and many others. I've done a lot of idiot things with Kristine, Avery, Josh, and Max. I've had some of the most fun roommates anyone could ask for, especially Claire, Bob, and Nina, and the rest have been awesome and understanding as well. I also thank the entire Holladay family, Lindsay, Meredith, Mallory and Ginny, and their parents Rick and Mary Beth for their support and love.

Finally, and most importantly, I want to thank my family, especially my parents Chris and Julie, and my brother and sister-in-law Mark and Robin, who have supported me through difficult times, while sharing joy in successes and fun times as well.

Preface

Portions of the text and data from this dissertation are reproduced from the following previously published work under fair use:

Nygren PJ, Scott JD. Therapeutic strategies for anchored kinases and phosphatases: exploiting short linear motifs and intrinsic disorder. Front. Pharmacol., 28 July 2015 | http://dx.doi.org/10.3389/fphar.2015.00158

Chapter 1: Introduction to AKAPs and phosphatase anchoring

Characterizing PKA anchoring

The cAMP-dependent protein kinase PKA was first identified and described by Edwin G. Krebs in 1968 as catalyzing the transfer of phosphate from ATP to a target serine or threonine residue in substrate proteins (Walsh et al., 1968). Since the initial identification of this ubiquitous kinase, many studies have defined its regulation by regulatory subunits (R-subunits), of which there are four isoforms (RIα, RIβ, RIIα, RIIβ) (Taylor et al., 2012). PKA regulatory subunits inhibit the activity of the PKA catalytic subunit (C-subunit) by occupying the substrate binding site of the C-subunit and preventing the phosphorylation of substrate proteins (Corbin et al., 1978). When cAMP binds to the R-subunits and inhibition is released, the C-subunit is able to assume its catalytic activity and phosphorylate nearby targets. In addition, each R-subunit isotype contains an N-terminal docking and dimerization domain (D/D domain) that is the basis for the formation of a heterotetramer composed of 2 R-subunits, each of which bind 1 C-subunit (2:2 stoichiometry)(Corbin et al., 1975;Newlon et al., 1999). In addition to the formation of R-subunit dimers, this D/D domain is responsible for docking to a genetically diverse but functionally related family of proteins called A-kinase anchoring proteins (AKAPs) (Scott et al., 1990;Newlon et al., 2001).

The first AKAP to be identified was microtubule-associated protein 2 (MAP2) by analysis of associated cAMP-dependent kinase activity (Theurkauf and Vallee, 1982). The number of AKAPs identified since has vastly increased due to use of a far-Western technique known as the RII overlay (Carr et al., 1991), as well as through more recent development of computational algorithms designed to predict R-subunit binding regions (Burgers et al., 2015). Some of the most characterized AKAPs include AKAP79/150, gravin, AKAP15/18, and mAKAP (Wong and Scott, 2004). In addition, some AKAPs have been shown to bind RI subunit isoforms, either with dual-specificity for RI and RII, or preference for the

RI types (Huang et al., 1997b;a;Lacana et al., 2002;Kovanich et al., 2010;Means et al., 2011). However, the majority of AKAPs interact primarily with RII isoforms.

AKAPs tether pools of readily stimulated PKA holoenzymes to subcellular compartments and organelles through a variety of mechanisms (Langeberg and Scott, 2015). Importantly, AKAPs also bind other signaling enzymes such as phosphodiesterases (PDEs), G-protein coupled receptors (GPCRs), ion channels, and protein phosphatases to form complexes that are able to integrate and modulate multiple second messenger signaling pathways and fine-tune cellular signaling responses. Many excellent reviews have described the range of binding partners these AKAPs associate with (Wong and Scott, 2004;Carnegie et al., 2009;Welch et al., 2010;Diviani et al., 2011;Sanderson and Dell'Acqua, 2011). In this introduction, I focus on the structural basis for anchoring of PKA as well as the protein phosphatases that oppose cAMP-mediated signaling.

Structural basis for PKA anchoring

Though AKAPs are not typically related to one another on a sequence level, a common unifying feature is their ability to bind the D/D domain of R-subunit dimers through a short (14-18 residues) amphipathic helix, which appears to have arisen relatively early in evolution (Peng et al., 2015). This helix is often one of the few ordered regions, as most AKAPs are intrinsically disordered (Gold et al., 2008). Therefore, this helix serves as a short linear motif (SLiM), an emerging concept in cellular signaling with important implications for protein-protein interactions and drug development (Van Roey et al., 2014). For example, a recent study examining the scaffolding properties of the yeast deubiquitinating enzyme Ubp10 showed that the interplay of SLiMs and intrinsic disorder is essential for facilitating interactions with diverse substrates and binding partners (Reed et al., 2015). SLiMs are often isolated within intrinsically disordered proteins and can serve to facilitate transient interactions which allows a single anchoring protein to interact with a dynamic range of signaling partners (Ren et

al., 2008). The first atomic model of an AKAP helix was solved using peptides derived from AKAP79 and Ht31 (AKAP-Lbc) (Newlon et al., 1999). It was obtained using NMR techniques and was solved in complex with the D/D domain (residues 1-44) of RIIα. Subsequently, other structures of the D/D domain in complex with various AKAP-derived helices have been solved using X-ray crystallography (Figure 1.1A) (Gold et al., 2006;Kinderman et al., 2006;Sarma et al., 2010). The D/D domain has been shown to adopt an anti-parallel four-helix X-type bundle that forms a platform with a hydrophobic groove. This groove is the basis for a high affinity interaction with the hydrophobic face of amphipathic AKAP helices. The D/D domain is then connected via a flexible linker to two cAMP-binding cassettes per protomer that display cooperative binding of cAMP (Vigil et al., 2004;Zawadzki and Taylor, 2004). Upon binding of cAMP, a conformational change occurs that relieves inhibition of the PKA C-subunit and allows it to phosphorylate nearby substrates. Crystal structures have been solved for the cAMP-binding cassettes in complex with C-subunit or with cAMP (Figure 1.1B) (Su et al., 1995;Diller et al., 2001;Wu et al., 2007;Zhang et al., 2012). Together with the known structure of the D/D in complex with AKAP helices, these structures have provided insights at the atomic level about the intricate topology and organization of the different functional elements of PKA holoenzyme.

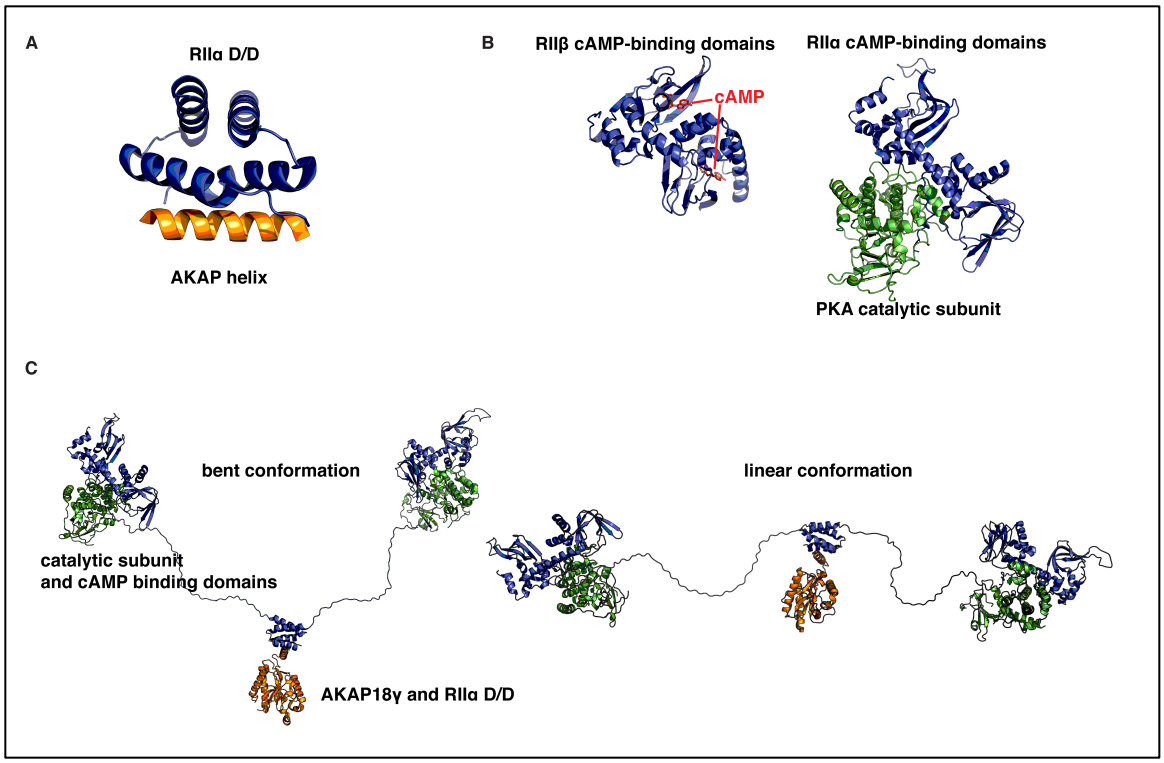

FIGURE 1.1. Structural basis for protein kinase A (PKA) holoenzyme formation and anchoring. (A) Crystal structure of the synthetic A-kinase anchoring protein (AKAP) helix AKAP's (orange) in complex with the RIIα docking/dimerization (D/D) domain, residues 1–44 (blue). The AKAP amphipathic helix binds to a hydrophobic groove created by the antiparallel X-type helix bundle of the RII D/D domain. PDB ID: 2IZX. (B) Left: RIIβ cAMP-binding cassettes (blue) in complex with cAMP (red). Right: RIIα cAMP binding cassettes in complex with PKA catalytic subunit (green). With cAMP bound at each of two sites, RII releases inhibition of the catalytic subunit. When cAMP is not present, RII presents an inhibitory sequence to the active site, preventing phosphorylation of PKA substrates. PDB IDs: 1CX4, 2WVS. (C) A pseudo-atomic model of the PKA holoenzyme in complex with AKAP18γ derived from low-resolution EM data. This illustrates that the PKA holoenzyme has a constrained range of flexibility (~300 Å) provided by AKAPs, allowing the catalytic subunits to be poised near potential substrates. PDB IDs: 3J4Q, 3J4R. Models were prepared using PyMol (Schrödinger).

Yet, there is currently no high-resolution structural information available for the 46 (in mammals) amino acid flexible linker that connects the D/D domain to the pseudosubstrate region that binds the C subunit and to the tandem cAMP binding cassettes. Therefore, a recent study used single particle electron microscopy

studies to examine the structure of an AKAP18γ-PKA holoenzyme complex (Smith et al., 2013). This study revealed that although many crystal structures of RII and C subunits showed surface contact between each heterodimer of RII and C, the complexes likely occupy a much broader conformational space that is constrained by the length of the linker, yet facilitated by the intrinsic disorder of the linker (Figure 1.1C). This linker-guided conformation sampling may be a mechanism by which PKA preferentially phosphorylates substrates within the same macromolecular complexes upon elevation of cAMP levels. cAMP phosphodiesterases (PDEs) have been suggested to form a 'fence' around subcellular pools of elevated cAMP (Baillie et al., 2005). AKAP18γ has been shown to form a complex with PDE4D3 and regulate its activity via PKA phosphorylation (Stefan et al., 2007). In combination with local restraint of PKA conformations by the RII flexible linker, these local PDE fences represent an intriguing scheme by which spatiotemporal specificity may be regulated by macromolecular signaling complexes.

Targeting the PKA/AKAP interaction for therapeutics

Since PKA activity modulates a variety of physiological events, such as cardiac remodeling, disrupting the PKA/AKAP interface has been a long-standing area of interest for therapeutics (Troger et al., 2012)(Table 1). One of the first disruptors of the AKAP/RII interaction is the 24 amino acid peptide Ht31, named after human thyroid clone 31, which was later realized to represent a biologically active segment of the multifunctional scaffolding protein AKAP-Lbc (Carr et al., 1992a). The Ht31 peptide has since been lipid modified with a stearic acid group to increase its membrane permeability for treatment of cell lines and elucidation of anchored PKA signaling events (Vijayaraghavan et al., 1997;Gold et al., 2012). *In silico* approaches have resulted in optimized peptides that mimic the AKAP amphipathic helix and bind to RII or RI with high affinity (Alto et al., 2003). Additionally, structure-based approaches have further increased the specificity of the peptide superAKAPis for RII to the low nanomolar affinity range with a

12,000-fold preference for RII over RI (Gold et al., 2006). Conversely, the RI-anchoring disruptor peptide (RIAD) has been engineered to specifically disrupt RI/AKAP interactions (Carlson et al., 2006). Several groups have developed peptidomimetics that imitate amphipathic helix structures and are able to disrupt RI/RII interactions with AKAPs (Schafer et al., 2013;Singh et al., 2014). Recent work has centered on developing stapled AKAP-mimetic peptides that are cell-permeable and have increased stability (Wang et al., 2014;Kennedy and Scott, 2015;Wang et al., 2015). These properties increase the utility of these peptides for therapeutic purposes as well as for molecular dissection of the mechanisms by which AKAPs influence local PKA signaling pathways.

Since there are numerous AKAPs and only four R-subunit isoforms, any disruptor that relies on an interaction with an R-subunit is by definition non-selective. In order to disrupt a specific AKAP's ability to bind PKA, anchoring disruptors must bind to an AKAP helix with high affinity and recognize the unique structural features of one AKAP helix preferentially. In order to select variants that exhibit preferential binding to specific AKAPs, a phage-display screening approach used immobilized AKAP helices to enrich for phage variants that displayed mutant RII D/D domains. These mutant D/D domains are termed Rselects, and have been shown in preliminary work to bind and label AKAPs in a cellular context as well as *in vitro* with purified proteins (Gold et al., 2013). Further development of these Rselects could lead to high affinity binding variants that could disrupt individual pools of anchored PKA while allowing other anchored PKA signaling events to proceed unperturbed. The potential to isolate spatially constrained post-translational modifications is an important step forward for targeted therapeutics. However, utility of this approach as a cell-based means of selectively interrupting particular PKA-AKAP interfaces has yet to be rigorously established.

Small molecule disruptors are another attractive means to pharmacologically target the PKA-AKAP interface. Although these studies are still in their formative

stages, there have been a few successful attempts at moderate-throughput screening for small molecule AKAP disruptors (Schachterle et al., 2015). Perhaps the most notable example is the development of 3,3'-diamino-4,4'-dihydroxydiphenylmethane (FMP-API-1), a small molecule antagonist that appears to allosterically inhibit the RII-AKAP interaction and activate anchored PKA C subunit (Christian et al., 2011). Despite extensive characterization of this compound, the mechanism of action of FMP-API-1 has yet to be defined. Nevertheless, the future is bright for the discovery and development of cell soluble chemical entities that target PKA-AKAP interfaces.

Protein phosphatase anchoring

Classically, protein phosphatases are considered to oppose the action of kinases, by removing phosphate groups from serine, threonine, or tyrosine residues. In addition, a burgeoning family of pseudokinases and pseudophosphatases are emerging as key players in cell signaling (Reiterer et al., 2014). Protein phosphatases fall into two main classes: serine/threonine phosphatases, and tyrosine phosphatases. While there are 428 serine/threonine kinases, there are only ~40 serine/threonine phosphatases (Moorhead et al., 2007). This disparity in gene number implies that additional mechanisms come into play as a means to modulate and vary the substrate specificity of these critical regulatory enzymes. Philip and Tricia Cohen were the first to recognize that regulation of protein phosphatases by association with regulatory and targeting subunits is a crucial mechanism to allosterically modulate substrate specificity (Stralfors et al., 1985;Cohen and Cohen, 1989). Others have shown that most of the three classes of serine/threonine phosphatases are modulated by targeting subunits (Langeberg and Scott, 2015). Here, I focus exclusively on protein phosphatase 1 (PP1) and protein phosphatase 2B (PP2B, or calcineurin), since these ubiquitous phosphatases often oppose the action of PKA and are especially reliant on anchoring for their regulation.

Protein phosphatase 1 regulation by auxiliary proteins

PP1 has an important role in a number of physiological processes, notably regulation of glycogen synthesis (Hubbard et al., 1990), nuclear events (Helps et al., 1998) and synaptic long term potentiation (LTP) and long term depression (LTD) (Morishita et al., 2001;Malinow and Malenka, 2002). The latter two events occur through phosphatase opposition of calcium/calmodulin-dependent kinase II (CaMKII) and PKA phosphorylation of glutamate receptors at the post-synaptic density. The PP1 catalytic subunit (PP1c) associates with over 200 regulatory subunits, many of which bind via a conserved short linear peptide motif called the RVxF motif (Cohen, 2002;Roy and Cyert, 2009).

Some of these subunits serve primarily to inhibit the catalytic activity, such as the protein Inhibitor 1 (I-1) and dopamine and cAMP-regulated phosphoprotein 32 (DARPP32)(Williams et al., 1986). Notably, some of these inhibitors are activated by PKA phosphorylation. Other regulatory subunits contain localization signatures that target PP1 to specific subcellular regions and may or may not also inhibit the enzymatic activity of PP1c. The most recognized examples of these targeting subunits are the myosin phosphatase targeting subunit MYPT1, the G_M regulatory subunit, p53-binding protein 2 (53BP2), and PP1 nuclear targeting subunit (PNUTS). Recent investigation of PNUTS has highlighted several properties shared by many PP1-binding proteins (Choy et al., 2014). First, the RVxF motif serves as a short linear interaction motif (SLiM) and is responsible for the primary interaction with PP1. Second, intrinsic disorder in PNUTS facilitates extended contact with PP1 on additional surfaces to fine-tune the phosphatase. Third, binding of PP1 to these surfaces inhibits its activity towards some substrates without physically blocking the active site of the phosphatase (Figure 1.2A).

A number of AKAPs have been shown to interact with PP1c, including D-AKAP1 (Steen et al., 2000), AKAP220 (Schillace and Scott, 1999), and yotiao (Westphal

et al., 1999). Likewise, some isoforms of AKAP18 are thought to sequester PP1, although it would appear that this occurs via indirect mechanisms (Singh et al., 2011). All direct PP1-AKAP interfaces utilize some version of the degenerate RVxF motif. D-AKAP1 was suggested to be involved in anchoring PP1 for efficient nuclear envelope reassembly after mitosis (Collas et al., 1999;Steen et al., 2000). AKAP220 has been shown to anchor PP1 through a modified KVxF motif, and this has been proposed to play a role in regulating the activity of glycogen synthase kinase 3β (GSK3β) through modulation of the phosphorylation state of serine 9. Phosphorylation of this residue results in suppression of GSK3β activity (Schillace et al., 2001;Tanji et al., 2002). Yotiao, a product of the AKAP9 gene, also contains an RVxF motif and has been shown to regulate the phosphorylation state of NMDA receptors through localization of PP1 (Lin et al., 1998;Westphal et al., 1999). AKAP18 does not appear to interact directly with PP1, but some reports indicate that it binds Inhibitor-1 to promote its phosphorylation by PKA (Singh et al., 2011). The net effect of this later phosphorylation event is to promote local inhibition of PP1c.

PP2B regulation by auxiliary proteins

PP2B, also known as calcineurin, is a broadly-expressed obligate heterodimeric protein phosphatase that is activated by calcium and calmodulin (Stewart et al., 1982). Like PP1, PP2B is involved in diverse processes such as synaptic plasticity (Mulkey et al., 1994), glucose metabolism (Hinke et al., 2012), cardiac signaling (Tandan et al., 2009), and immune responses (Clipstone and Crabtree, 1992). In addition, activation of PP2B can mobilize a phosphatase cascade, through dephosphorylation of PP1 regulatory subunits (Mulkey et al., 1994). The catalytic A subunit of PP2B contains an autoinhibitory region that occludes the active site in the absence of calcium. Upon elevation of calcium levels, calcium ions bind directly to the regulatory B subunit and to calmodulin, which in turn interacts with the autoinhibitory region and allows PP2B to resume catalytic activity towards phosphosubstrates (Li et al., 2011). Because calcium transients

often envelop the whole cell rather than occurring locally, regulation of PP2B's activity towards substrates is accomplished primarily through protein-protein interactions. The best-known PP2B substrate is the nuclear factor of activated T-cells (NFAT) family. These transcription factors contain phosphoserine-rich regions and, when dephosphorylated, dimerize and translocate to the nucleus, where they are responsible for controlling a range of transcriptional responses such as inflammation in response to immune system signaling (Li et al., 2012). The common immunosuppressants FK506 and cyclosporine target PP2B and mediate their primary effect through inhibition of NFAT signaling (Liu et al., 1991).

Not only is NFAT a typical PP2B substrate, it also contains two SLiMs, which are both typical of PP2B interacting proteins – the PxIxIT motif and the LxVP motif (Roy et al., 2007;Rodriguez et al., 2009). The PxIxIT motif forms a beta strand that binds to a hydrophobic groove formed by a beta sheet on the PP2B A subunit (Li et al., 2007). This surface of the PP2B A subunit is analogous to the region of PP1 which interacts with the RVxF motif (Figure 1.2A). Proteins that contain PxIxIT motifs include NFAT, regulator of calcineurin 1 (RCAN1) (Mehta et al., 2009), TWIK-related spinal cord potassium channel (TRESK) (Roy and Cyert, 2009) and notably, AKAP79/150 (Dell'Acqua et al., 2002). The LxVP motif is a degenerate sequence that binds to the interface of the A and B subunits of PP2B, and only binds to activated calcineurin (Rodriguez et al., 2009). It has been challenging to describe a consensus LxVP sequence. Therefore, many LxVP motifs have been identified without originally being aware of their identity. The first LxVP motif to be described was that of the RII subunit by Edwin Krebs and colleagues in 1986 (Blumenthal et al., 1986), although it was not recognized as a conserved binding mode until it was found in NFAT. Many substrates of PP2B contain an LxVP motif, and it has been suggested that all efficient substrates contain some type of sequence that interacts with the LxVP binding region on PP2B (Grigoriu et al., 2013). The characterization of multiple SLiMs that interact with various surfaces of PP2B parallels that of PP1, and suggests other shared

mechanisms, such as fine-tuning the location and activity of PP2B through a combination of disorder and SLiMs. Recently, a structure of PP2B in complex with a viral inhibitor peptide from African swine fever revealed the binding site for the LxVP motif in atomic level detail (Grigoriu et al., 2013). This crystal structure reveals that the leucine residue occupies a pocket formed by two aromatic residues, and when these are mutated to alanine residues they no longer interact with the LxVP motif. In addition, this binding site overlaps with the binding sites for cyclosporine and FK506 complexes (Figure 1.2B). However, no structure has been solved of the PP2B heterodimer bound to calmodulin in the fully active state, so the question of how LxVP motifs are able to impact PP2B activity remains unclear.

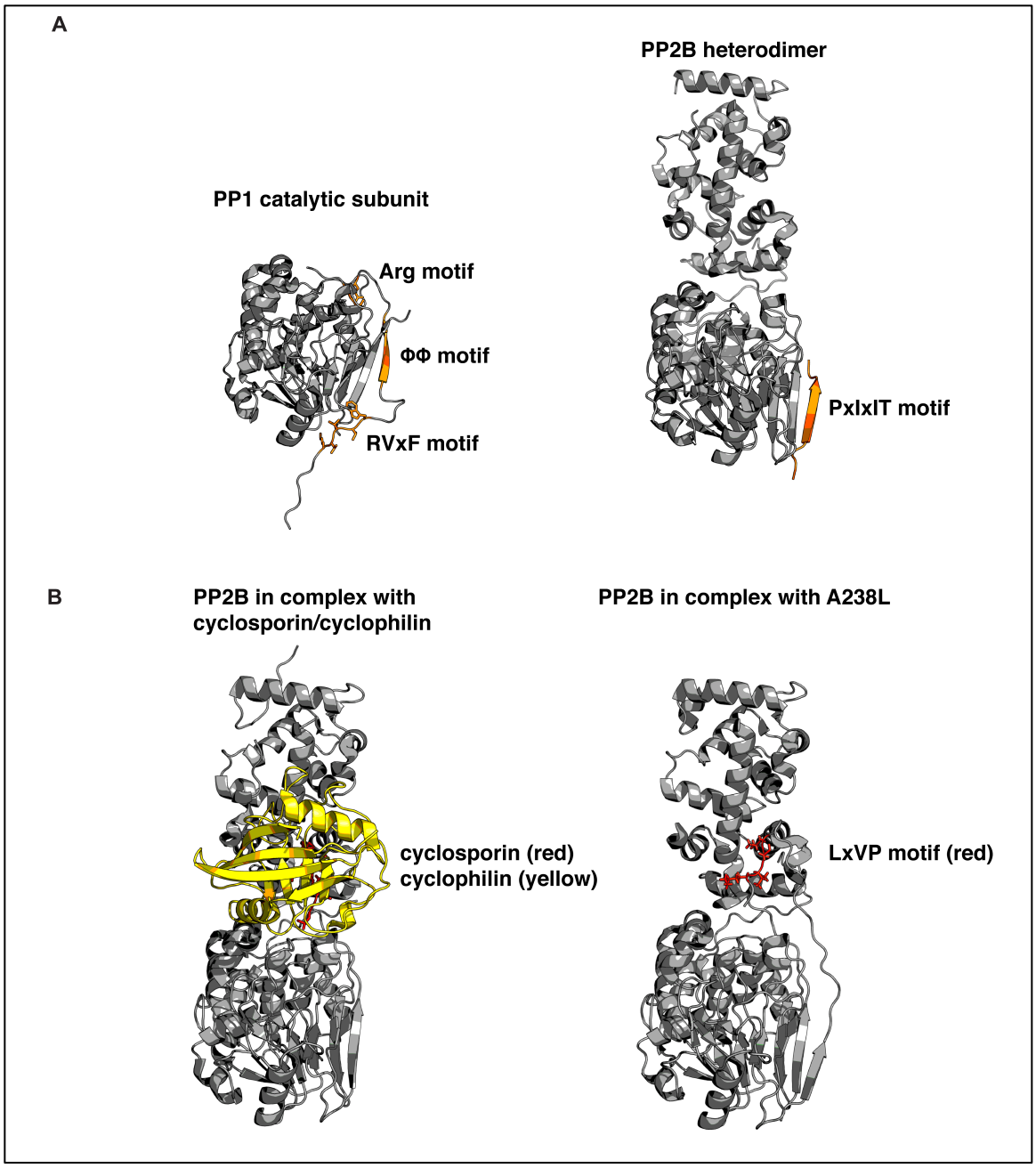

FIGURE 1.2. Structural basis for phosphatase regulation and anchoring. (A) Left: PP1 catalytic subunit (gray) in complex with RVxF and auxiliary anchoring motifs from protein phosphatase 1 (PP1) nuclear targeting subunit (PNUTS; orange). Right: PP2B (gray) in complex with PIAIIIT sequence from AKAP79 (orange). Comparison reveals that similar surfaces are used for anchoring, and that multiple motifs can simultaneously interact with varied portions of the molecule. PDB IDs: 4MOY, 3LL8. (B) Left: PP2B in complex with cyclosporin (red)/cyclophilin (yellow) complex. Right: PP2B in complex with a viral peptide A238L, containing a PxIxIT motif, as well as an LxVP motif (red). Cyclosporin and

LxVP peptides bind to overlapping surfaces on PP2B, formed by both the catalytic and regulatory subunits of PP2B. This surface does not occlude the active site of the phosphatase, yet immunosuppressants are able to allosterically inhibit PP2B activity toward substrates. PDB IDs: 1MF8, 4F0Z. Models were prepared using PyMol (Schrödinger).

Some AKAPs have been shown to bind PP2B, including the aforementioned AKAP79 and mAKAP (Li et al., 2010). In addition, the AKAP gravin has been suggested to be in the same complex as PP2B and beta-adrenergic receptors, however, evidence for a direct interaction is not immediately apparent (Shih et al., 1999). The mAKAP interaction has been mapped to the residues 1286-1345 in the mAKAPα splice variant. However, this region does not contain an easily identifiable PxIxIT or LxVP sequence. Loss of mAKAP-PP2B binding was shown to result in reduced cardiac myocyte hypertrophy in response to norepinephrine, as well decreased atrial natriuretic factor expression. Interestingly, the pool of PP2B bound to mAKAP appeared to be active, and required to dephosphorylate NFAT efficiently in response to phenylephrine treatment. Formation of the PP2B/mAKAP complex was enhanced in vitro by calcium/calmodulin, suggesting that the interaction may occur via a similar mechanism to the LxVP motif (Li et al., 2010).

AKAP79 is perhaps the best characterized AKAP, and its interaction with PP2B has been extensively investigated. Although original studies suggested an interaction site was restricted to the N-terminal third of AKAP79 (Coghlan et al., 1995), later work described the primary site of interaction as being a PxIxIT motif from residues 337-343 (Dell'Acqua et al., 2002;Oliveria et al., 2007). Use of a transgenic mouse model in which AKAP79 lacks this region, known as the AKAP79ΔPIX mouse, has revealed that AKAP79-anchored PP2B is required for NMDA-dependent hippocampal long-term depression and NFAT signaling in neurons (Oliveria et al., 2007;Sanderson et al., 2012). Intriguingly, the AKAP79ΔPIX mouse shows improved insulin sensitivity, indicating that this

interaction may be a possible therapeutic target for Type II diabetes (Hinke et al., 2012).

Because of the importance of the AKAP79-PP2B interaction, much emphasis has been placed on understanding the structural basis of this interaction. Native mass spectrometry and biochemical approaches have suggested an additional interaction site for PP2B between residues 1-153 of AKAP79 that is dependent on calcium/calmodulin (Gold et al., 2011). Although a crystal structure of PP2B in complex with a synthetic PxIxIT motif was solved in 2007 (Li et al., 2007), the first structure of PP2B bound to a natural PxIxIT motif was that of AKAP79 (Li et al., 2012). This structure matched closely with the previously solved structure, in that crystal packing is such that each PIAIIIT sequence contacts two PP2B A subunits along the PxIxIT binding region. This, along with native mass spectrometry approaches, raises the question of whether AKAP79 is capable of binding two PP2B molecules simultaneously.

Because of PP2B's importance in a range of physiological contexts, there is great interest in developing disruptors that target specific PP2B anchoring proteins (Table 2). One of the first targeted approaches resulted in an optimized high-affinity PxIxIT motif called the VIVIT peptide (Aramburu et al., 1999), which is the aforementioned synthetic peptide that was co-crystallized with PP2B. In addition, fluorescence polarization screens for small molecules that disrupt binding to the PxIxIT motif have yielded a potential candidate known as INCA-6 that is able to inhibit PP2B-NFAT signaling with similar potency to cyclosporine and FK506, but through an alternate mechanism (Kang et al., 2005). Recently, an approach disrupting the LxVP interaction in macrophages through lentiviral expression of an LxVP peptide was shown to reduce inflammation and confer resistance to arthritis and contact hypersensitivity (Escolano et al., 2014). Understanding the molecular basis for PP2B anchoring has led to potential for therapeutics and the realization that primary and secondary binding sites may both be targeted for

diverse physiological effect. Because the AKAP79-PP2B interaction is important in many processes, specifically targeting this interaction may be of great promise.

PKA phosphorylation events and the phosphatases that oppose these events are tightly regulated by anchoring proteins. Recently, the use of new and sophisticated biochemical, biophysical, and structural techniques has forged two important concepts. First, the combination of SLiMs and intrinsic disorder allow anchoring proteins to allosterically and spatially control the range and specificity of phospho-signaling. Second, AKAPs are not just static anchors, but are conformationally and compositionally flexible. This allows them to adapt to a varied and continually changing cellular signaling environment. A recent paper characterizing binding partners of the AKAP ezrin by quantitative mass spectrometry revealed that conformational switches in ezrin are accompanied by changes in the complement of enzymes present in the complex (Viswanatha et al., 2013). This may well prove to be the case for many AKAPs allowing them to perform cell-type specific roles. Moreover, the concept of AKAPs as conformational switches could account for how the same anchoring protein can simultaneously perform distinct functions at multiple locations within a single cell.

These new biological insights have been demonstrated by using hybrid structural techniques such as x-ray crystallography, NMR, hydrogen/deuterium exchange experiments and crosslinking/mass spectrometry (Burns-Hamuro et al., 2005;Gold et al., 2011;Choy et al., 2014). The advent of direct electron detectors for cryo-electron microscopy has increased attainable resolutions (Campbell et al., 2012), and will likely contribute to increased structural understanding of these flexible multi-protein complexes. In addition, computational advances in understanding heterogeneous cryo-EM samples will also advance our knowledge of multiple conformational states (Behrmann et al., 2015). Already, negative-stain approaches such as random conical tilt (RCT) experiments are allowing researchers to understand structural heterogeneity in protein complexes (Veesler

et al., 2014). Combining these approaches with biosensors for enzymatic activity (Mehta et al., 2014;Mehta and Zhang, 2014) will provide a more comprehensive picture of how the structural properties of anchored kinase and phosphatase complexes are able to influence local signaling in a cellular context. Finally, as exemplified by a recent structure-guided pharmacophore screen for inhibitors of PP2B anchoring, atomic resolution structural insights will guide design of small molecules that target anchoring protein interactions in the context of short linear motifs and intrinsic disorder (Matsoukas et al., 2015).

My research takes advantage of hybrid structural techniques including electron microscopy (EM), crosslinking-mass spectrometry approaches (XL-MS), and biophysical characterization of multiple interaction sites to characterize an activity-dependent conformational switch that occurs in the AKAP79-PP2B complex upon activation of the phosphatase. I describe the first structure of an AKAP-phosphatase complex and show that active PP2B forms a secondary interaction with AKAP79 via an LxVP-type motif, Additionally, using Förster resonance energy transfer (FRET) reporters for PP2B activity, I find that the LxVP motif contained in AKAP79 is important for fine-tuning phosphatase activity within anchored complexes. This work contributes significantly to our understanding of how disordered proteins can contribute to a balance between dynamic and tonic interactions thereby fine-tuning enzyme activity.

Chapter 2: Purification and electron microscopy of AKAP79/PP2B

Introduction:

AKAP79 (AKAP150 in rodents, AKAP75 in bovine, gene designation AKAP5) was originally identified and cloned by Charles Rubin, and was the first PKA-binding protein to be designated an AKAP (Sarkar et al., 1984;Hirsch et al., 1992). AKAP79 was the first AKAP shown to interact with both kinases and phosphatases (Coghlan et al., 1995). The opposing actions of the kinases PKA and protein kinase C (PKC), and the phosphatase PP2B have been well characterized in a variety of physiological systems. In addition, AKAP79 has been shown to integrate multiple second messenger signaling pathways, such as cAMP- and calcium-mediated signaling. AKAP79 is localized to the plasma membrane by three membrane binding basic regions (MBBR A, B, and C), as well as by palmitoylated cysteine residues in the N-terminal third of the molecule (Dell'Acqua et al., 1998;Delint-Ramirez et al., 2011). Through these sets of anchored enzymes, AKAP79 is able to regulate ion channels such as the CaV1.2 calcium channel (Hall et al., 2007;Oliveria et al., 2007), the KCNQ potassium channel (Hoshi et al., 2003), and the GluA1 subunit of the AMPA receptor (Colledge et al., 2000;Lu et al., 2007). Other studies have also shown that AKAP79 can regulate TRPV1 channels (Schnizler et al., 2008;Brandao et al., 2012), NMDA receptor subunits (Dell'Acqua et al., 2006), and Kv channels (Nystoriak et al., 2014). These characteristics are often shared by members of the AKAP family, and together with the large body of literature regarding AKAP79, make AKAP79 an attractive target for studying general principles of anchoring proteins.

AKAP79 is named for its apparent molecular weight as measured by SDS-PAGE, however, its predicted molecular weight is approximately 49 kDa, and this has

been confirmed by mass spectrometry approaches. Purified AKAP79 expressed in insect cells or bacterial expression systems appears to have no post-translational modifications by mass spectrometry (Gold et al., 2011), although previous studies have shown that AKAP79 can be lipid modified for membrane localization (Delint-Ramirez et al., 2011;Keith et al., 2012) and phosphorylated for unknown function (Dell'Acqua et al., 1998). The human form of the protein is 427 amino acids in length, while the mouse and rat forms (known as AKAP150) are 745 and 714 amino acids, respectively, due to an inserted repeat region of unknown function. Hereafter, all numbering and descriptions will refer to the human form, unless otherwise noted.

The PKA binding helix of AKAP79 resides near the C-terminus of the molecule, at residues 391-408 (Carr et al., 1992b). PP2B binds through a modified PxIxIT motif (PIAIIIT) located at residues 337-343 (Oliveria et al., 2007). Other direct interactions that have been well characterized include PKC (residues 31-52) (Klauck et al., 1996), calmodulin (residues 31-52) (Faux and Scott, 1997), the membrane-associated guanylate kinase (MAGUK) family members SAP97 and PSD-95 (unknown binding region) (Colledge et al., 2000), and the L-type calcium channels (C-terminal leucine zipper) (Altier et al., 2002). In addition, AKAP79 has been shown to bind F-actin, cadherin, PIP2 phospholipids and adenylyl cyclases (Dell'Acqua et al., 1998;Gorski et al., 2005;Efendiev et al., 2010;Willoughby et al., 2010). It is clear that a small protein is unlikely to interact with all of these binding partners simultaneously, therefore it has been suggested, and shown in some cases, that AKAP79 complexes exist in compositionally diverse forms within a cell (Hoshi et al., 2005). Many physiological studies have indicated an important role for AKAP79-anchored PP2B, which in some cases has been shown to be more important for regulation of ion channels and signaling events than even PKA anchoring. A long-standing question has been how PP2B and Ca2+/calmodulin-dependent protein kinase II (CaMKII) are differentially activated: they often have opposing action on a shared substrate, yet are both activated by

calcium and calmodulin (Barria et al., 1997a;Barria et al., 1997b). Therefore, understanding the molecular mechanism of PP2B anchoring is of great interest.

The first study describing PP2B anchoring by AKAP79 suggested that an N-terminal peptide, which was able to inhibit phosphatase activity *in vitro*, was involved in the binding interaction (Coghlan et al., 1995). However, later studies pointed towards the region spanning residues 315-360, while the modified PxIxIT motif contained within this region was shown to be particularly crucial for binding (Oliveria et al., 2007).

The importance of the PxIxIT motif in AKAP79 has been underscored by numerous studies, biochemical as well as physiological. In particular, a transgenic mouse model in which the PxIxIT motif has been deleted has been shown to improve glucose clearance and increased insulin sensitivity. This model recapitulated the results seen in a global AKAP150 KO mouse, indicating that anchored PP2B played a more crucial role in this signaling pathway than other anchored enzymes did (Hinke et al., 2012). Similarly, a series of knockdown experiments using AKAP150-directed siRNA in rat brain slices showed deficits in hippocampal NMDA-receptor dependent long-term depression (LTD) that could be rescued by constructs deficient in PKA binding but not by constructs unable to bind PP2B (Jurado et al., 2010). Again, this underscored the important role for PP2B in regulating ion channel activity through dephosphorylation of local substrates.

This AKAP79 PxIxIT sequence contains an additional isoleucine that is not found in most other PxIxIT motifs in nature. Structural studies showed that this caused Ile-338 to occupy the binding pocket on PP2B that was typically occupied by the first proline in other PxIxIT motifs (Li et al., 2007;Li et al., 2012). In addition, this peptide forms a beta strand that has hydrophobic residues on both sides of the strand, whereas most other PxIxIT peptides found in nature have hydrophobic

residues on only the side which interacts with PP2B (Aramburu et al., 1999;Roy and Cyert, 2009). This gave rise to the hypothesis that AKAP79's PxIxIT motif may be able to interact simultaneously with two protomers of PP2B. While this hypothesis was also supported by crystal packing in the structure of PP2B with AKAP79's PIAIIIT sequence, it has remained unclear whether this occurred in solution and *in vivo* (Li et al., 2012).

A native mass-spectrometry experiment estimated the size of an AKAP79/PP2B/CaM/RII D-D complex to be 466 kDa. This suggested that AKAP79 formed a dimer, each protomer binding two PP2B molecules. In addition, crosslinking and collision-induced mass-spectrometry have also suggested that AKAP79 is capable of forming dimers (Gold et al., 2011). However, it is also known that AKAP79 is prone to aggregation when expressed as an untagged protein in bacterial or insect cells. Therefore, the possibility remains that these results are artifacts of such a preparation, or that AKAP79 exists in a state of equilibrium between dimer and monomer.

This study also suggested that an additional binding site was present. Three fragments of AKAP79 were expressed and purified as GST fusion proteins (residues 1-153, 154-296, 297-427). These immobilized fragments were incubated with purified Flag-PP2B under basal conditions, or with calcium and calmodulin supplemented. Surprisingly, PP2B bound not only to a fragment comprised of residues 297-427 (which contains the PxIxIT domain), but also to a fragment comprising residues 1-153 exclusively in the presence of calcium/CaM (Gold et al., 2011). Because of this evidence suggesting a dynamic bipartite interaction, I investigated the structural basis for this complex by purifying an AKAP79/PP2B/CaM complex under calcium or EDTA conditions, and used a single particle electron microscopy approach called random conical tilt (RCT), which is designed to characterize multiple conformations.

RCT is a low-resolution EM technique that is very powerful for resolving global structural changes. Images are collected of negatively stained particles in an untilted view, and a large (45-60˚) tilted view (Veesler et al., 2014). Individual particles are selected, correlated to their untilted views, and then aligned to one another and computationally separated into different classes based on their similarity to one another. Angular information about the view of each particle is inferred by 1) the rotation needed to align the particles into classes, and 2) the known angle of the sample in the tilted images. The angular information is then used to create a separate 3-D reconstruction for each class. These 3-D reconstructions can be used to tell whether particular classes correspond to different views of the same conformation or to conformational variability with the complex.

Results:

To understand the topology and architecture of AKAP79 complexes, I first conducted bioinformatic analyses of the primary structure of the anchoring protein using algorithms designed to predict disorder and locate potential short linear motifs (Figure 2.1A). Analysis of the AKAP79 sequence using the IUPred (Dosztanyi et al., 2005a;b) and PONDR (Li et al., 1999) disorder prediction algorithms identified extended regions of disorder, especially in the first ~350 amino acids (Figure 2.1B and 2.1C). Conversely, the C-terminal portion of AKAP79 is predicted to be more ordered (Figure 2.1B and 2.1C). This is consistent with experimental and structural evidence showing that this region contains the PKA-binding helix (blue) that is required for high affinity interaction with the regulatory subunits of the PKA holoenzyme (Sarkar et al., 1984). The ANCHOR (Dosztanyi et al., 2009;Meszaros et al., 2009) and SLiMPred programs (Mooney et al., 2012) search for motifs within disordered regions that are predicted to adopt static conformations upon association with protein binding partners. Both algorithms identified regions corresponding to the known binding sites for protein kinase C/calmodulin (green), and PP2B (yellow). Other potential

short linear motifs of unknown function were also evident, including a prominent peak between residues 122 to 136 of the anchoring protein (Figure 2.1D and 2.1E).

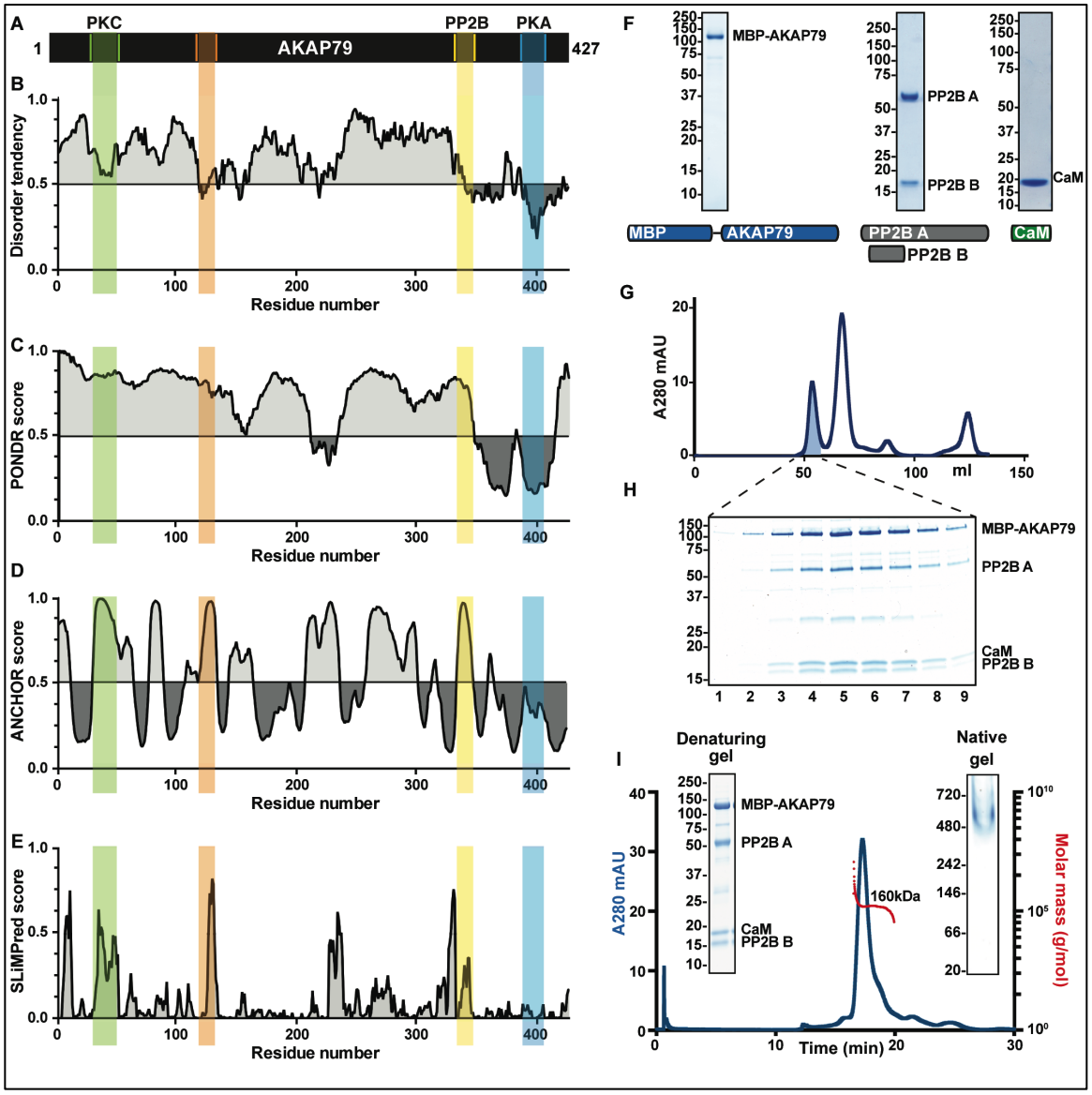

FIGURE 2.1. Characterizing disorder and short linear motifs in AKAP79 complexes. (A) Primary topology of AKAP79, with well-described binding sites notated and aligned to subsequent figures. (B) IUPred prediction of disordered regions of AKAP79. (C) PONDR prediction of disordered regions of AKAP79 (D) ANCHOR prediction of short linear interaction motifs in AKAP79. (E) SLiMPred prediction of short linear interaction motifs in AKAP79. (F) Coomassie gels and constructs used to purify individual subunits of an MBP-AKAP79/PP2B/CaM complex. (G) Gel filtration of a fully assembled complex of MBP-AKAP79/PP2B/CaM. (H). Coomassie gel of the peak containing the full complex. (I) SEC-MALS of MBP-AKAP79/PP2B/CaM. A280 in blue, molecular weight measurement in red. Denaturing and native gels confirming presence of all subunits migrating as a single complex.

In order to empirically determine whether selected AKAP79-enzyme macromolecular assemblies adopt a range of conformations, I purified individual components of an AKAP79/PP2B/CaM complex (Figure 2.1E). AKAP79 was expressed in *E. coli* as a His tagged-MBP fusion protein and purified on nickel resin (Figure 2.1F). A bicistronic plasmid was used to express the PP2B subunits (GST-PP2B A and PP2B B) in bacteria. The phosphatase holoenzyme was purified on glutathione sepharose (Figure 2.1F). Likewise GST-calmodulin was expressed and purified in a similar manner (Figure 2.1F). In both cases the GST tags were removed by cleavage with PreScission Protease (GE Life Sciences). MBP-AKAP79 was incubated with molar excesses of PP2B and CaM and the complex was isolated by gel filtration chromatography. The elution profile for this complex on a Superdex 200 column suggested an extended configuration of the complex, rather than a folded globular conformation (Figure 2.1G). SDS-PAGE analysis confirmed that the first peak contained all expected subunits (Figure 2.1H). I performed size-exclusion chromatography with inline multi-angle light scattering measurements (SEC-MALS) to show that the molecular weight of the complex corresponds to a 1:1:1:1 ratio of subunits (~160 kDa), although it migrates on gel filtration where a globular protein of ~450-550 kDa would (Figure 2.1I). Denaturing SDS-PAGE confirmed that this peak contains all subunits, and when the isolated complex is applied to native PAGE, it migrates with the same pattern as a 480 kDa globular protein, lending further support to the hypothesis that AKAP79 complexes exist in a disordered non-globular state (Figure 2.1I).

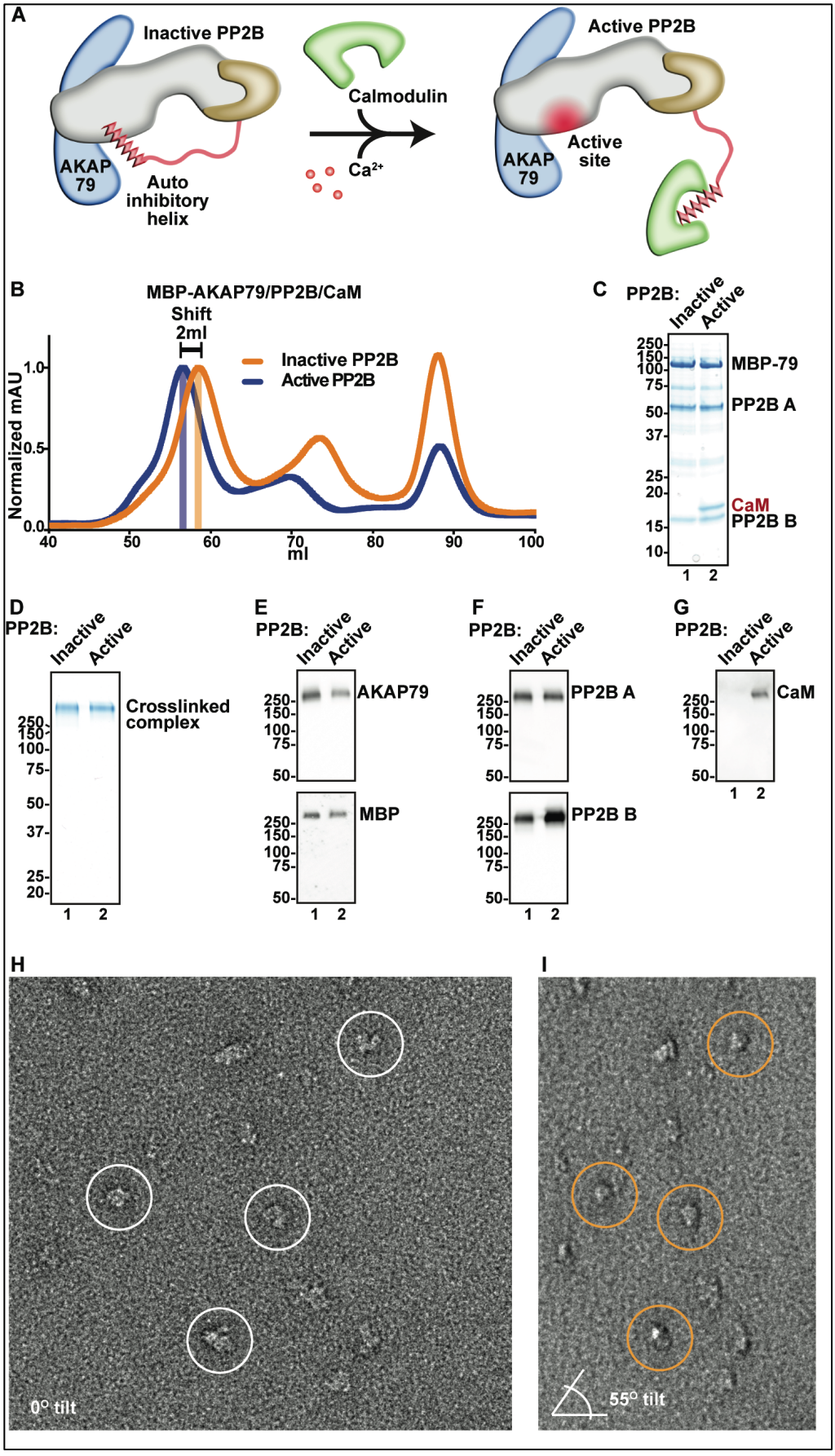
A
Inactive PP2B
Calmodulin
Active PP2B
AKAP 79
Auto inhibitory helix
Ca2+
Active site
B
MBP-AKAP79/PP2B/CaM
Shift 2ml
Inactive PP2B
Active PP2B
Normalized mAU
ml
C
PP2B:
Inactive
Active
MBP-79
PP2B A
CaM
PP2B B
D
Crosslinked complex
E
AKAP79
MBP
F
PP2B A
PP2B B
G
CaM
H
0° tilt
I
55° tilt

FIGURE 2.2. Analysis of compositional and conformational changes in the presence and absence of calcium. (A) Schematic showing structural rearrangement and relief of PP2B autoinhibition upon addition of calcium and calmodulin. (B) Comparison of identical MBP-AKAP79/PP2B/CaM complex preps obtained in the presence (blue) or absence (orange) of calcium. (C) Coomassie gel of pooled peak fractions showing lack of CaM in the inactive complex form. (D) GraFix purification and crosslinking stabilizes complexes into single bands as visualized on coomassie gels. (E) Western blots for MBP and the c-terminal region of AKAP79 confirm incorporation of full-length protein. (F) Western blots of PP2B A and B subunits confirm incorporation. (G) Western blot for CaM confirms that it is only present in the active form of the complex. (H) Example micrographs of the inactive complex in untilted and tilted views. Sample particles have been marked to illustrate correlation between the two views.

PP2B is autoinhibited by a helical segment of the A subunit and, upon binding of calcium and activated calmodulin, a conformational change occurs that relieves this inhibition and allows substrates to access the active site (Figure 2.2A)(Li et al., 2011). This structural rearrangement is not well understood; therefore I investigated whether there were changes in the overall conformation and composition of the AKAP79/PP2B/CaM complex. Complexes were assembled as before in the presence of calcium or in the presence of EDTA. I observed a 2 mL shift in the elution profile of the complex in the presence of EDTA, indicating a possible conformational or compositional change (Figure 2.2B). SDS-PAGE analysis of the peak fractions showed that calmodulin is no longer present in the complex when calcium has been chelated (Figure 2.2C). This confirmed that compositional changes were occurring. I wanted to investigate possible conformational changes, however the flexibility of the complex proved refractory to crystallographic screens, so I used single particle EM studies.

I used a random conical tilt (RCT) approach to characterize these complexes with electron microscopy. Early attempts to prepare negatively stained samples suggested that the complex was dissociating upon application to EM support grids. Therefore, I used a modified gradient fixation (GraFix) approach to stabilize the complex (Kastner et al., 2008;Stark, 2010). I applied complexes purified by

gel filtration to a 5-30% w/v continuous glycerol gradient that was also a 0-0.15% glutaraldehyde crosslinker gradient. This provided more stringent purification and separation from aggregates and partial complexes. In addition, it facilitated isolation of crosslinker-stabilized complexes that migrates as a single band on SDS-PAGE (Figure 2.2D). I performed western blots on these complexes to confirm that each expected subunit was present (Figure 2.2E-G). As expected, the inactive complex did not contain CaM (Figure 2.2G). I then applied the samples to grids and stained using 2% uranyl formate. I acquired tilt-pair images of these samples at 0˚ (Figure 2.2H) and -55˚ angles (Figure 2.2I). The micrographs for each complex showed particles that are approximately 15 nm in diameter. Individual particles were selected, aligned, correlated to their tilted pairs, and used as the basis for 3-D reconstructions (Figure 2.2H-I).

I obtained reference-free class averages and, over several iterations, used these to discard unsuitable particles that were auto-picked (edges of artifacts, small subcomplexes, etc). After class averages of sufficient quality were obtained, I chose a representative set of templates to use for reference-based alignment. The results of this alignment were used to make 3-D models.

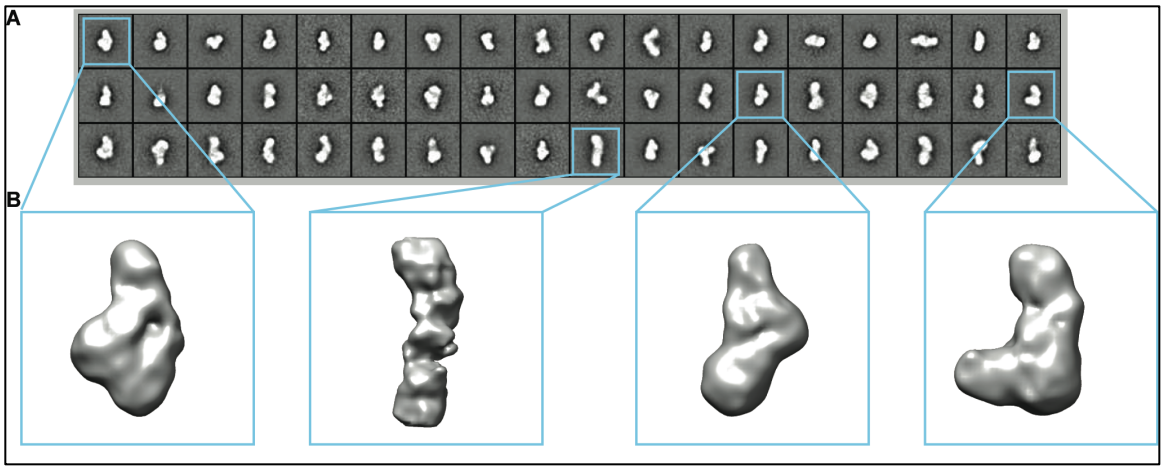

FIGURE 2.3. Random conical tilt analysis of inactive complexes. (A) Reference-based class averages of the complex obtained by negative stain EM. (B) Sample 3-D models of MBP-AKAP79/PP2B illustrating representative states of the complex, from extended to more compact.

For the inactive form of the complex, the class averages obtained from reference-based alignment suggested that the complex adopts a range of conformations from extended to more compact (Figure 2.3A). The RCT models derived from each class had resolutions ranging from ~50-80 Å. The quality of reconstructions was reliable, as indicated by the fact that individual particles were properly aligned and classified, and that the models built from tilted views closely resembled the class averages from the untilted views (Figure 2.3B). In addition, the size of the complexes were consistent with our MALS measurements indicating that this complex exists in a 1:1 ratio of AKAP79:PP2B.

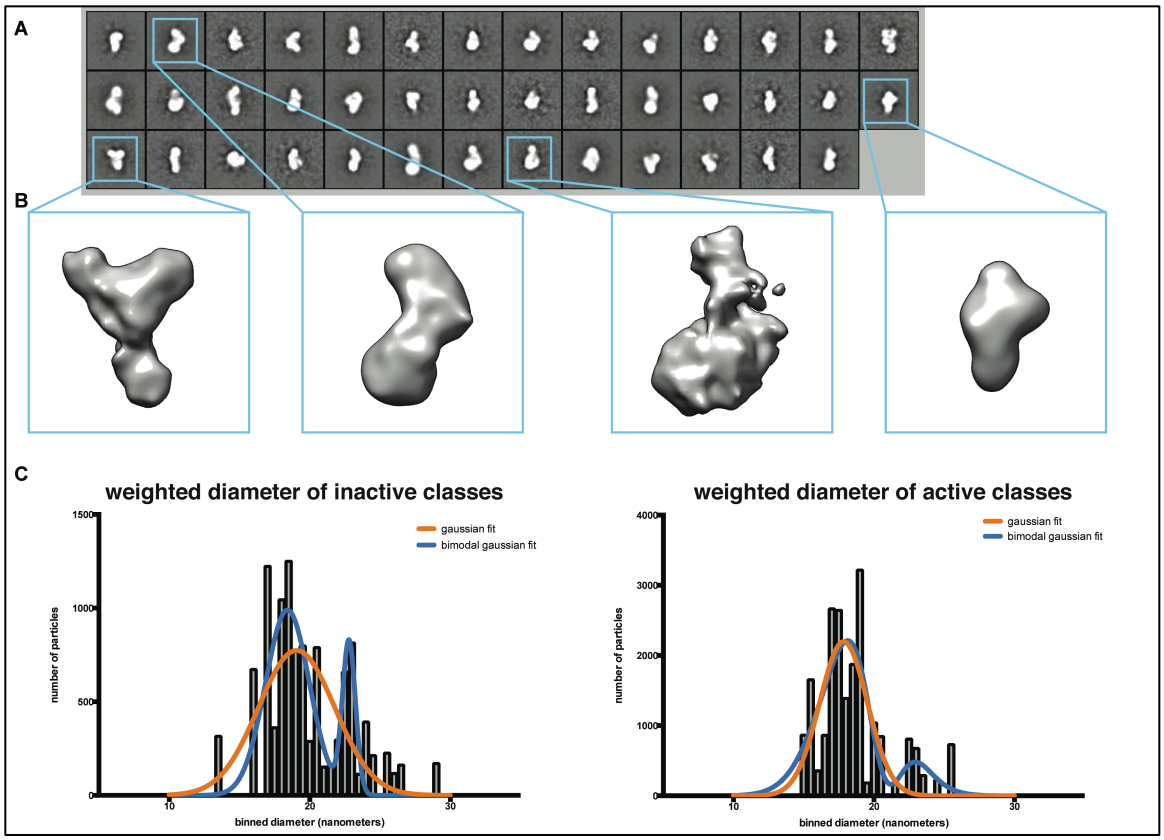

FIGURE 2.4. Random conical tilt analysis of active complexes and comparison to inactive complexes. (A) Reference-based class averages of the complex obtained by negative stain EM. (B) Sample 3-D models of MBP-AKAP79/PP2B/CaM illustrating representative states of the complex, from extended to compact. (C) histogram plots of class diameters, fit with gaussian or sum of gaussian curves.

The active form of the complex also yielded good quality RCT models (Figure 2.4A). It appears that this form adopts some similar conformations as the inactive form of the complex (Figure 2.4B). In addition, docking of the known crystal structures of PP2B, CaM, and MBP into the density map suggests that AKAP79 does not adopt a globular conformation. This is supported by the fact that in many conformations there is unaccounted for density, but not enough for a globular protein.

Visual comparison of the class averages obtained suggests that the inactive form is more likely to adopt an extended conformation, while the inactive form is more

likely to be compact. This is consistent with the knowledge that an additional binding site is generated upon activation of PP2B. I measured the largest diameter of each class and then weighted these diameters by the number of members in each class. I then plotted the values on a histogram and fit either a Gaussian curve or the sum of two Gaussian curves to the histogram. This allowed me to test whether there were multiple populations of conformational states. I found that the inactive form had both a larger overall mean diameter, and also contained a larger population that was in a more extended form (Figure 2.4C).

Discussion:

This work represents the first structural models of AKAP79 complexes, and also characterizes the flexibility and disorder inherent in the complex. We show that predictions of disorder and SLiMs align closely with known binding sites and regions of secondary structure in AKAP79. In addition, there are at least two prominent predicted short linear motifs that have not been well characterized, one of which I will describe in the following chapter (residues 122-136). Because intrinsic disorder is often important to the function of proteins, especially anchoring proteins, my characterization of multiple conformational states of AKAP79 has implications for its function and regulation of binding partners.

Use of the GraFix preparative technique allowed me to stabilize a flexible complex for EM analysis, and the analysis shows that conformational flexibility is not removed by this crosslinking step. In addition, visual comparison of the two states of the complex seems to suggest that the inactive state is more likely to assume an elongated form, while the active state covers a range of conformations that is more compact. This could be explained by reports of an additional site of contact between PP2B and AKAP79 located in the N-terminal third of AKAP79 (Coghlan et al., 1995;Gold et al., 2011). The range of conformational space that this complex occupies is likely facilitated by the

intrinsic disorder of AKAP79. This is a similar concept to the recent work done characterizing an AKAP18-PKA holoenzyme complex by EM. This study showed that intrinsic disorder in the complex facilitated a constrained range of motion, allowing PKA to exert its enzymatic activity on nearby substrates in a precisely tuned manner (Smith et al., 2013). Therefore, it is important to determine the role of AKAP79 in tuning the activity of its interacting kinases and phosphatases.

In addition, the active form of the complex seems to preferentially occupy closed conformational states and likely utilizes multiple phosphatase targeting motifs. This is similar in concept to anchoring of PP1, and is likely important for directing a non-specific phosphatase towards specific substrates under specific cellular signaling conditions. For example, a long-standing question in neuronal signaling has been the relative activity of CaMKII and PP2B in response to postsynaptic influxes of calcium. Both enzymes are activated by calcium/CaM, and have many overlapping substrates, but obviously have opposite effects on the phosphorylation state of substrates such as the GluA1 subunit of the AMPA receptor, the NMDA receptor and other postsynaptic targets.

Use of negative stain and random conical tilt techniques have allowed low-resolution characterization of multiple conformational states. However, it remains unclear exactly how each subunit is arranged in these states. While docking of crystal structures into the EM density maps allows guesses at where the subunits are localized, more sophisticated approaches will facilitate confident subunit mapping. Future work on these complexes will first focus on localizing subunits within the EM models using Fab fragments of antibodies directed towards each subunit. These antibodies will be complexed with AKAP79/PP2B/CaM complexes and then analyzed by EM to obtain class averages. These class averages will be compared to those obtained without Fab fragments to localize the subunits in the EM models.

In addition, assembly of larger complexes including the PKA holoenzyme have been performed. These larger complexes containing additional subunits may be suitable for cryo-electron microscopy. Use of the deleted linker RII construct that was developed for EM studies of AKAP18 could help align images properly, given advances in direct electron detectors and alignment of low contrast, noisy images that are inherent in cryo-EM (Campbell et al., 2012;Campbell et al., 2014;Campbell et al., 2015).

Chapter 3: Identification and characterization of an LxVP motif in AKAP79

Introduction:

The original study describing the AKAP79-PP2B interaction identified a region of AKAP79 that appeared to have similarity to FKBP12, and a series of lysine and arginine residues. This was located between residues 88-102 of AKAP79. A peptide corresponding to this region was shown to inhibit PP2B activity, although the mechanism of this inhibition was unclear (Coghlan et al., 1995). In addition, as mentioned before, there appear to be global changes in the conformation that are instigated by activation of PP2B in the presence of calcium and CaM, and generation of an N-terminal binding site for PP2B on AKAP79 (Gold et al., 2011). Therefore, I hypothesized that AKAP79 may contain a site similar in mechanism to an LxVP motif.

As briefly mentioned, previous studies of the structural basis for LxVP anchoring include a computational prediction of the complex of PP2B and the NFATc1 LxVP motif (Roy et al., 2007). In addition, a crystal structure of a virally derived peptide in complex with PP2B was solved and used to predict a binding model of the RII LxVP motif on PP2B (Grigoriu et al., 2013). This LxVP motif seems to serve as a secondary binding site in many cases, as most PP2B interacting proteins also contain PxIxIT motifs. This is a similar concept to PP1 anchoring proteins that often utilize multiple short, medium affinity motifs to interact with distinct surfaces of the phosphatase to form an overall stronger interaction. Previous studies have implicated the LxVP motif in optimally positioning phosphoresidues for efficient dephosphorylation (Roy and Cyert, 2009;Escolano et al., 2014). This is supported by studies showing that PP2B activity towards phosphopeptide substrates is diminished in the presence of LxVP peptides, while PP2B activity towards small molecule substrates such as pNPP and diFMUP is enhanced (Rodriguez et al., 2009). The proposed model is that LxVP peptides

stabilize an active conformation of the enzyme; they also occupy a crucial binding interface for many PP2B substrates found in nature.

This also explains the molecular basis for the efficacy of the immunosuppressants cyclosporine and FK506. Both of these form complexes with immunophilin proteins that bind to the same interface as the LxVP motif, and inhibit PP2B activity towards NFAT, likely by competing directly with the LxVP motif present in NFAT (Rodriguez et al., 2009). Therefore, I used chemical crosslinking, mass spectrometry, structural modeling, peptide array approaches, AlphaScreen protein-protein interaction assays, and mutational analysis to probe the molecular basis for the N-terminal interactions with AKAP79.

Results:

I purified MBP-AKAP79/PP2B/CaM complexes and then incubated with either 5 mM $CaCl_2$ or 5 mM EDTA overnight. After gel filtration to isolate these complexes, the complexes were crosslinked, trypsin digested, and subjected to mass spectrometry analysis to identify crosslinked peptides.

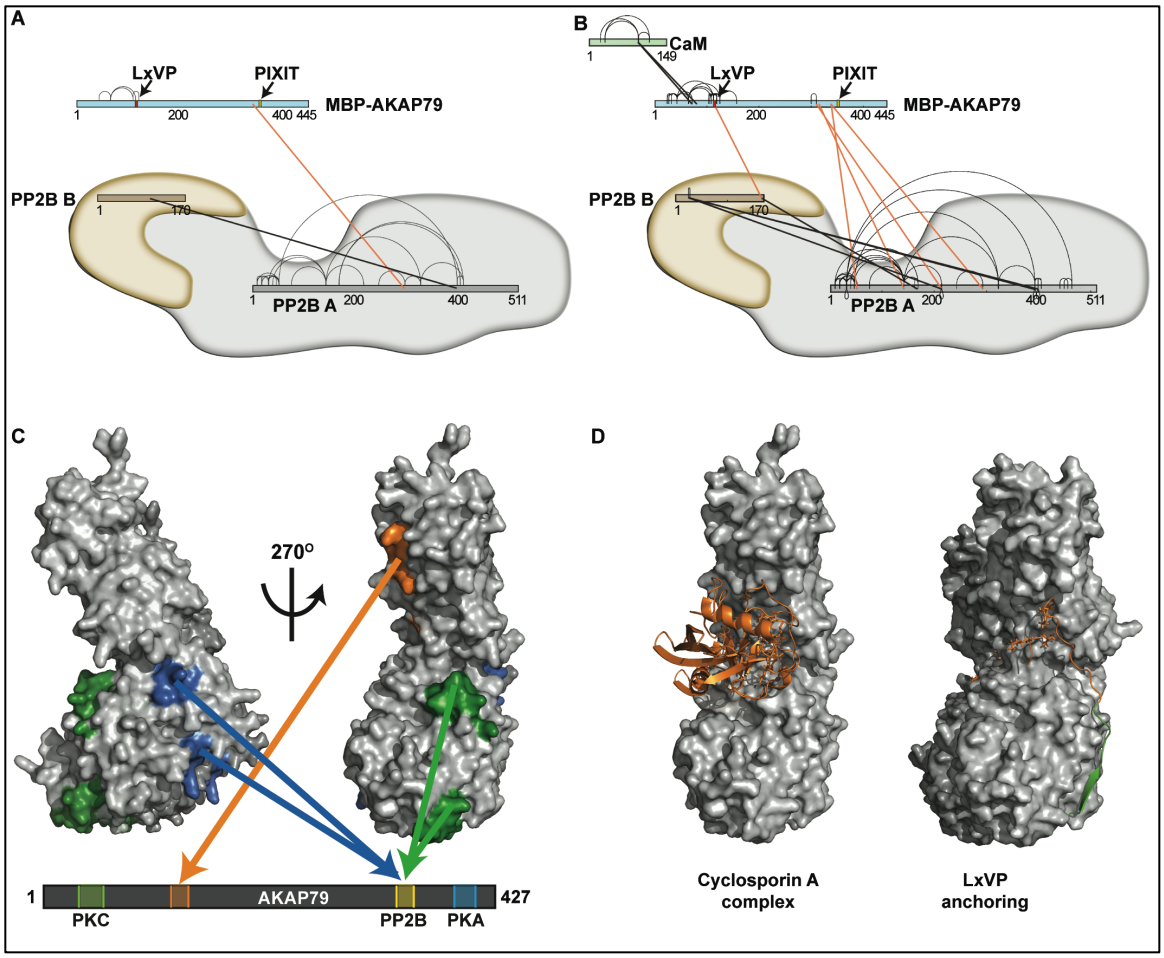

FIGURE 3.1. Crosslinking/mass-spectrometry of AKAP79/PP2B interactions. (A) Crosslink map of residues observed in EDTA conditions. Thick lines indicate intermolecular crosslinks, and orange lines indicate crosslinks from PP2B to AKAP79. (B) Crosslink map of residues that were observed in calcium conditions. Thick lines indicate intermolecular crosslinks, and orange lines indicate crosslinks from PP2B to AKAP79. (C) Colored patches indicate intermolecular crosslinks between PP2B and AKAP79 mapped onto the crystal structure of PP2B (PDB: 1MF8). Arrows indicate where these residues crosslinked on the primary sequence of AKAP79. (D) Comparison of structures of PP2B in complex with cyclosporine/cyclophilin (PDB: 1MF8), or the A238L viral peptide containing an LxVP motif (PDB: 4F0Z), showing the overlap in binding surfaces.

I mapped these peptides onto the primary sequences of the subunits (Figure 3.1A and B). As expected, PP2B crosslinked near the PxIxIT motif of AKAP79 under both conditions. A unique crosslink between AKAP79 and PP2B was observed in the calcium condition. This crosslink was between residue 113 of

AKAP79 and residue 165 of PP2B B subunit. This peptide is shown in orange on the structure of PP2B (Figure 3.1C). In addition, I mapped the other intramolecular crosslinks onto the structure of PP2B and observed that they are close to the known binding site for the PxIxIT motif. Comparison of these crosslinks with the structures of PP2B in complex with cyclosporine/cyclophilin or an LxVP peptide shows that the unique binding site appears to occupy the same surface of the molecule. This is consistent with the mode of calcium-sensitive interaction being via an LxVP motif, since it overlaps with the known binding site.

In order to more precisely determine whether LxVP motifs competed for the same binding surface on PP2B as the N-terminal interaction site does, I used fragments of AKAP79 corresponding to residues 1-153, 154-296, and 297-427, termed N, M, and C, respectively (Figure 3.2A). I expressed these fragments as GST fusions and immobilized them on glutathione beads. I then incubated them with purified Flag-tagged PP2B in the presence or absence of calcium/CaM or the presence of the NFATc1 LxVP peptide or a scrambled control. As expected, the C fragment interacted with PP2B in all cases, since this interaction relies on the PxIxIT motif, which is not sensitive to calcium, and does not occupy the same surface as the LxVP peptide. The M fragment did not interact in any cases, and the N fragment only interacted in the presence of calcium/CaM. This N-terminal interaction was successfully competed away by the LxVP peptide, but not by the scrambled control (Figure 3.2 B). This indicates that the N-terminal interaction is a *bona fide* LxVP interaction. I also carried out phosphatase assays on the same samples using a small molecule substrate (diFMUP) so that the presence of the LxVP motif would not interfere with the ability of PP2B to display activity towards the substrate. The results of this assay mostly mirrored the amount of PP2B pulled down, although it appeared that in the C fragment samples, there was a slight increase in activity upon addition of the LxVP peptide (Figure 3.2 C).

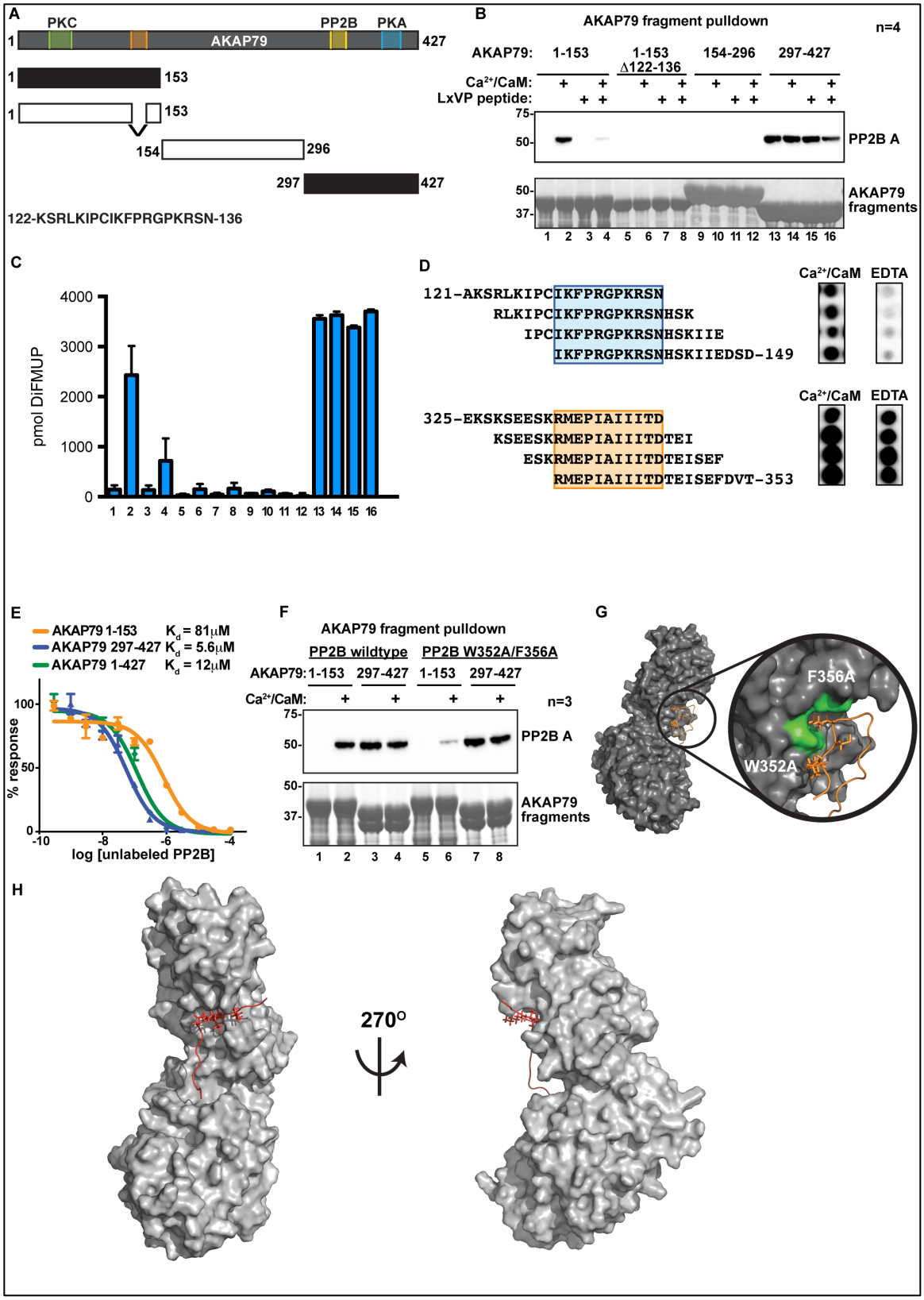

FIGURE 3.2. Mapping and characterization of the LxVP binding interfaces for AKAP79 and PP2B. (A) The fragments of AKAP79 used in subsequent

experiments. (B) GST-AKAP79 fragment precipitations of Flag PP2B in the presence of calcium and calmodulin, and competition with an LxVP peptide. Lanes 5-8 show deletion of a putative motif abolishes binding. (C) Phosphatase activity assays of the samples from panel B against a small molecule, diFMUP. (D) Overlay of peptides that exclusively bound PP2B in the presence of calcium/calmodulin (top) compared to the PxIxIT motif. (E) AlphaScreen competition assay to calculate Kd values for interactions between PP2B and full-length AKAP79 (green), or fragments of AKAP 79 (C – blue, N – orange). (F) Mutations were made to PP2B that are predicted to abolish the LxVP binding pocket. GST fusion protein precipitations were used to test whether this mutant could bind to the N-terminal fragment of AKAP79. (G) Structural model showing PP2B (gray) with the mutated residues (green) interacting with an LxVP motif (orange). (H) CABS-dock prediction of a likely binding site for AKAP79 122-136 (red) overlaps with the known LxVP binding pocket.

Because crosslinking-mass spectrometry experiments showed a unique crosslink under PP2B activation conditions, I hypothesized that this peptide represented an LxVP motif. In addition, ANCHOR and SLiMPred algorithms predict that this peptide is a SLiM (Figure 2.1D and E), and sequence alignments showed a high degree of conservation. Finally, this sequence contained a four amino acid segment, LKIP, which is similar to the LxVP consensus motif. Therefore, I deleted this sequence in the context of the N-terminal fragment. Upon deletion of this motif, I observed a loss of binding to the N-terminal sequence (Figure 3.2B), and a similar loss of associated phosphatase activity (Figure 3.2C). This experiment showed that residues 122-136 were necessary for binding of PP2B to the N-terminal fragment of AKAP79.

I then tested whether this sequence was sufficient to bind PP2B *in vitro* by synthesizing 20-mer peptides that stepped by 4 residues down the entire sequence of AKAP79. I overlaid these peptide arrays with PP2B in the presence or absence of calcium/CaM. The sequence corresponding to the LxVP motif only bound PP2B in the presence of calcium/CaM, while the sequence corresponding to the PxIxIT motif overlaid with PP2B in both conditions (Figure 3.2D)

I then used an AlphaScreen protein-protein interaction assay to determine the binding affinity of PP2B for various fragments of AKAP79. This assay relies on conjugating purified biotin-PP2B to streptavidin donor beads, that when excited, release singlet oxygens that are able to diffuse a short distance in solution and excite a nickel acceptor bead that is conjugated to His-tagged AKAP79 fragments. This assay therefore relies on the interaction of PP2B and AKAP79 to give a signal. Untagged PP2B was used to compete away the interaction in order to approximate the Kd values. I found that the N-terminal fragment had a lower affinity (81 μM) than the C-terminal fragment (5.6 μM), which was similar to the binding affinity of the full-length protein (12 μM) (Figure 3.2E). This indicates that the PxIxIT motif is likely the primary binding determinant, while the LxVP motif is an auxiliary interaction.

Previous structures of PP2B in complex with LxVP motifs suggest that two aromatic amino acids (W352 and F356) are important for forming a binding pocket for the LxVP motif (Rodriguez et al., 2009). I mutated both of these residues to alanines and used the mutant form of PP2B in the same GST protein-protein interaction assay format as before. I found that the mutant form had reduced binding to the N-terminal fragment of AKAP79, while still interacting normally with the C-terminal fragment (Figure 3.2F and G)). Together, these results indicate that the binding surface on PP2B for the N-terminal fragment of AKAP79 is the same as the LxVP motif, and that the mode of interaction is the same.

As a final test of whether the peptide I identified from AKAP79 was likely to interact with PP2B in the same manner as LxVP motifs, I used the CABS-dock server to computationally predict the structure of AKAP79 122-136 in complex with PP2B (Blaszczyk et al., 2015;Kurcinski et al., 2015). The lowest energy conformation was assumed to be the most accurate and showed overlap with the

LxVP binding site and the binding pocket that was previously mutated (Figure 3.2H).

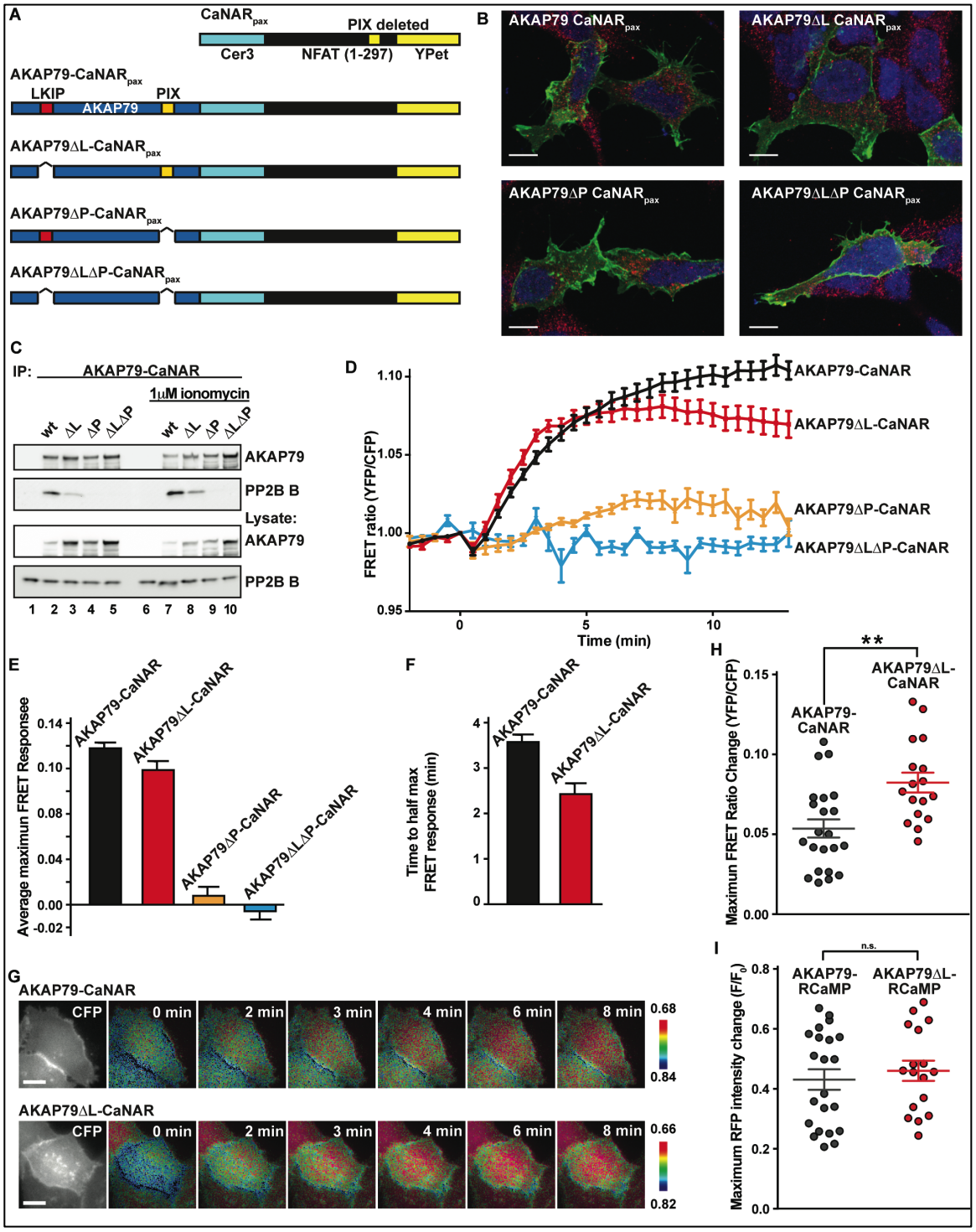

FIGURE 3.3. Use of AKAP79-CaNAR biosensors for anchored PP2B activity reveal that AKAP79 fine-tunes PP2B sensitivity towards physiological ranges of calcium. (A) Schematic of the fusion biosensors designed and used in this study.

(B) Confocal images of AKAP79-CaNAR variants (green), PP2B (red) and DAPI (blue) showing proper trafficking of various mutants. (C). Co-immunoprecipitation of PP2B with AKAP79-CaNAR variants under basal (lanes 1-5) and ionomycin treated (lanes 6-10) conditions. (D) Time course of FRET ratio signal upon stimulation with 1 μM ionomycin at t=0. (E) Average maximum FRET responses summarized by AKAP79-CaNAR variant. Columns 1 and 2 are not significantly different. (F) Kinetics of FRET responses to 1 μM ionomycin as described by time to half-max response. Columns 1 and 2 are significantly different. (G) Representative frames of FRET movies comparing wild-type AKAP79-CaNAR with AKAP79ΔLxVP-CaNAR signals. Colors are representative of the ratio value as described by the key to the right of each row. (H) Treatment of cells with 100 nM ionomycin reveals differences in the max response of each variant. (I) Use of the calcium indicator RCaMP shows that changes in max response are not due to differences in cellular calcium levels.

In order to test for functional effects of the bipartite interaction between AKAP79 and PP2B on anchored substrates, I took advantage of a FRET biosensor for PP2B activity called calcineurin activity reporter (CaNAR) (Mehta et al., 2014;Mehta and Zhang, 2014). I designed a series of modifications to this reporter, first making alanine mutations to the PxIxIT motif contained in the reporter itself to show that this was sufficient to abolish FRET responses to increases in intracellular calcium (see methods). This variant was termed the CaNARpax variant. This loss of FRET responses was rescued by fusing a C-terminal fragment of AKAP79 that contained the PxIxIT motif to the N-terminus of CaNAR. Next I designed a series of full-length AKAP79-CaNAR reporters that either had both binding sites, were lacking the LxVP site, or the PxIxIT site, or had both PP2B-binding sites deleted (Figure 3.3A).

Because the LxVP motif partially overlaps with a region that has been implicated in membrane trafficking, we used confocal fluorescent imaging to confirm that each variant was trafficked normally. All four variants localized to the membrane in HEK293 cells (green), while PP2B had similar cytoplasmic localization in all cases (red) (Figure 3.3B).

In order to assess whether changes in FRET signal were due to differences in the ability of the AKAP79-CaNAR reporters to interact with PP2B, I carried out co-immunoprecipitation experiments in HEK cells (Figure 3.3C). Cells were lysed under basal conditions (lanes 1-5) or after 10 minutes stimulation with 1 μM ionomycin (lanes 6-10). As expected from previous studies, and from my AlphaScreen approximation of affinities, loss of the PxIxIT motif caused a complete loss of interaction, while the deletion of the LxVP motif caused a decrease but not a complete loss. There seemed to only be a small change in the amount of PP2B recruited upon stimulation with ionomycin, indicating that as suspected, the PxIxIT motif is a tonic interaction.

FRET ratios were measured in HeLa cells after stimulation with 1 μM ionomycin (Figure 3.3D). Both constructs lacking the PxIxIT sequence did not respond to ionomycin treatment, which is consistent with co-immunoprecipation experimental results. The wild-type and ΔLxVP constructs both gave robust responses over the course of 20 minutes. The ΔLxVP construct plateaued more quickly and reached a slightly lower average maximum response. Statistical analysis of the maximum responses indicated that the difference between wild-type and ΔLxVP constructs was not significantly different (Figure 3.3E). However, it appeared that the speed at which the constructs responded varied. Analysis of the time to half-maximal response showed that there was a statistically significant difference (Figure 3.3F). This is especially evident at the 3- and 4-minute time points in the frame-by-frame comparison (Figure 3.3G). I hypothesized that these changes in speed were due to increased sensitivity to lower levels of calcium by the ΔLxVP variant.

In order to test whether this was the case, a new set of experiments was carried out in which the max response was measured after application of a 10-fold lower concentrations of ionomycin (Figure 3.3H). We also used the calcium indicator RCaMP (Akerboom et al., 2013) to ensure that the changes in max response

were not due to changes in the overall level of cellular calcium (Figure 3.3I). In this experiment, the ΔLxVP construct had a significantly higher maximum response, indicating that the LxVP motif serves to desensitize PP2B towards low levels of calcium, while allowing PP2B to still maintain maximal activity at higher levels of calcium. Therefore, the LxVP motif in AKAP79 serves to fine-tune PP2B sensitivity towards a range of calcium levels.

Discussion:

This portion of my project leverages hybrid structural techniques such as chemical crosslinking and mass spectrometry, and combines them with powerful biochemical and functional approaches, such as structure-guided mutagenesis, molecular docking/modeling, and the use of custom FRET biosensors for anchored phosphatase activity. I characterized a new binding site for PP2B on AKAP79, showed that this site is an LxVP motif, and investigated the interplay between the dynamic LxVP motif, and the tonic PxIxIT binding site.

Importantly, this LxVP site is located squarely within a region of AKAP79 that is predicted to form a SLiM (Chapter 2). Characterization of the binding affinities indicated that the PxIxIT motif is the primary determinant of binding. This is expected, as mouse models and previous biochemical studies have shown that loss of the PxIxIT motif is sufficient to completely disrupt binding to PP2B. Therefore, the LxVP motif is analogous to the MyPhonE or SILK motifs in PP1, while the PxIxIT motif is similar to the RVxF motif (Roy and Cyert, 2009). The combination of multiple binding motifs for a single enzyme allows fine-tuning of binding affinities under different enzymatic states, while also possibly influencing substrate selectivity.

Other proteins that have LxVP motifs have been shown to use them for various purposes. For example, the LxVP motif in RII was shown to be part of the minimal requirement for efficient dephosphorylation by Ed Krebs (Blumenthal et

al., 1986). NFAT family members use the LxVP motif to stimulate dephosphorylation of phosphosites located between the LxVP motif and the PxIxIT motif (Roy and Cyert, 2009). The scaffold protein KSR2 appears to only have an LxVP motif and this promotes dephosphorylation of upstream distal serine and threonine residues (Grigoriu et al., 2013). Because of the flexibility inherent in the LxVP motif, it is likely that most proteins contain regions of disorder surrounding the LxVP motif that act analogously to the disorder in RII, allowing a range of nearby phosphosites to occupy a constrained yet flexible conformational space so multiple sites can be dephosphorylated by a single anchored PP2B molecule.

My experiments involving the AKAP79-CaNAR FRET reporters addressed this concept by tethering AKAP79 to an artificial substrate and testing whether anchored PP2B could efficiently dephosphorylate local targets. The results of these experiments clearly show that AKAP79 can target PP2B to local substrates with full efficacy. Surprisingly, I found that the LxVP motif in AKAP79 actually attenuates PP2B's response to low levels of calcium, while maintaining its readiness to respond to local "floods" of calcium, such as those facilitated by the NMDA receptors and/or the L-type calcium channels in the postsynaptic density. Therefore, the LxVP motif in AKAP79 may be a possible mechanism regulating the different responses of PP2B and CaMKII to calcium stimulation during long-term synaptic plasticity events.

In addition, recent studies have implicated neuronal pools of AKAP79-anchored PP2B in dephosphorylation of NFAT in response to calcium entry via the L-type calcium channel (Oliveria et al., 2007;Li et al., 2012). Because NFAT dephosphorylation is the major target of the immunosuppressants cyclosporine and FK506, this raises the intriguing possibility that AKAP79-anchored PP2B may respond differently to immunosuppressants than cytosolic PP2B does,

thereby allowing some transcriptional events to occur in neurons, while being suppressed in immune cells.

Future experiments would help shed light on what physiological substrates might be regulated by AKAP79's LxVP motif. Obvious examples include the L-type calcium channel, NFAT, AMPA receptor subunits, and possibly AKAP79 itself. Technically challenging, but conceptually simple experiments could involve measurement of AMPA receptor currents in the context of AKAP79 KO neurons rescued with viral expression of AKAP79 mutants lacking various PP2B binding domains. In addition, SiteScan (MIT) predicts several phosphosites on AKAP79 that have unknown function but could be regulated by PP2B. There is also a possibility that AKAP79-anchored PP2B regulates the MAGUK proteins SAP97 and PSD-95. In summary, there are a variety of possible targets that could be regulated by the LxVP motif I have characterized in this work.

Chapter 4: Experimental methods

Bioinformatic predictions

For all predictions, the amino acid sequence of human AKAP79 was used. Disorder predictions were obtained using default parameters on IUPred (iupred.enzim.hu) and PONDR (pondr.com) (Li et al., 1999;Dosztanyi et al., 2005a;b). Predictions of short linear interaction motifs were obtained using ANCHOR (anchor.enzim.hu) and SLiMPred (bioware.ucd.ie) (Dosztanyi et al., 2009;Meszaros et al., 2009;Mooney et al., 2012). Graphs were prepared using Prism 6.0 (GraphPad Software).

Protein expression and purification

All proteins were transformed and expressed in BL21 (DE3) pLysS cells (Life Technologies). AKAP79 was expressed as an MBP fusion in a modified pMAL c5x backbone (NEB) in which the TEV cut site was replaced with a site recognized by Prescission protease (GE Life Sciences). In addition, a 10x His-tag was placed at the C-terminus of the AKAP79 sequence. AKAP79-transformed BL21 cultures were grown in Terrific Broth (Sigma) until OD600 = ~0.5, and expression was then induced with 0.4 mM IPTG at 37˚C for 4 hours. Cells were then pelleted, frozen at -20˚C and thawed and resuspended in 30 mL/liter of culture Buffer A (200 mM NaCl, 20 mM HEPES, pH 7.5) 4 mg/ml lysozyme, 1 mM AEBSF, 2 µg/ml leupeptin, 16 µg/ml benzamidine. After resuspension, Triton X-100 was added to 0.5%, and benzonase (Sigma-Aldrich) was added at a 1:20,000 dilution. After incubation for an additional 30 minutes, the lysate was cleared by spinning at 20,000 rpm in an SA-600 rotor (Sorvall) for 30 minutes. Clarified lysate was incubated with nickel affinity resin (Roche) for 1 hour, and then allowed to flow through by gravity. 2 mL wash/elution fractions were collected and analyzed by coomassie staining containing the following concentrations of imidazole: 10, 20, 30, 50, 75, 100, 250, 500 mM (x5). Fractions containing MBP-AKAP79 were then combined and concentrated to <5 mL and

applied to a HiLoad 16/600 Superdex 200 gel filtration column for separation at 0.5 mL/min. The peak corresponding to soluble MBP-AKAP79 was pooled and concentrated and flash-frozen, then stored at -80˚C.

GST-PP2B was cloned into the pGEX-6P1 backbone as a bicistronic expression vector containing a Shine-Dalgarno sequence between the A subunit and the B subunit. Calmodulin was also expressed as a GST fusion in the pGEX-6P1 vector. PP2B and calmodulin were both purified by affinity chromatography, the GST tag was cleaved and gel filtration chromatography was performed as described previously (Gold et al., 2011).

Complexes were formed by incubating 1 mg of MBP-AKAP79 with PP2B and CaM in a 1:2.5:3 molar ratio overnight in 20 mM HEPES, pH 7.5, 200 mM NaCl, and either 2 mM $CaCl_2$ or 2 mM EDTA. These samples were then injected onto to a Superdex Increase 200 10/300 column (GE) using an AKTApurifier FPLC using the same buffer they were incubated in overnight. Peaks were analyzed by SDS-PAGE and coomassie staining. The first peak, which elutes after the void volume, was pooled for further experimental analysis.

Light scattering

The SEC-MALS system was an AKTApure FPLC (GE), with an on-line Optilab T-Rex refractometer (Wyatt), and a Dawn Heleos II light scattering instrument (Wyatt). 500 µl of purified complex (~2 mg/mL) was injected onto a WTC-050S5 SEC column (Wyatt) and eluted at 0.5 mL/min directly into the on-line MALS instruments. Data was collected and processed to determine molecular mass using Astra 6 (Wyatt).

Crosslinking and native PAGE

Samples were stabilized for native PAGE analysis by crosslinking with 250 µM BS3 (Sigma) for 30 minutes at room temperature. The crosslinking reaction was

quenched by addition of Tris, pH 8.0 to 0.5 mM. The sample was then applied to NativePAGE 4-16% Bis-Tris gels (Life Tech.) according to the manufacturers instructions.

Grafix preparation

In order to prepare AKAP79/PP2B/CaM complexes for EM analysis, ~2 mg purified complex was concentrated to ~100 µL and applied to a continuous density/glutaraldehyde gradient. This gradient was prepared as described previously, with 5-30% (w/v) glycerol and 0-0.15% glutaraldehyde (Kastner et al., 2008;Stark, 2010). Samples were spun in an SW41Ti rotor (Beckmann-Coulter) at 35,000 rpm for 18 hours at 4˚C. The gradients were fractionated in ~200 ul aliquots and analyzed by SDS-PAGE. Fractions that contained a single stabilized band were selected for further analysis.

Western blotting

All western blots were performed by transferring samples from SDS-PAGE gels to nitrocellulose membranes at 1.00A for 36 minutes. Membranes were blocked in 5% milk in TBS/T plus 0.02% sodium azide. The following primary antibodies were used – mouse monoclonal anti-MBP-HRP 1:1000 (NEB), mouse monoclonal anti-FLAG-HRP 1:4000 (Sigma), rabbit polyclonal anti-AKAP79 C-terminus (Millipore), rabbit polyclonal anti-PP2B A subunit (Millipore), mouse monoclonal anti-PP2B B subunit (Abcam), and rabbit polyclonal anti-CaM (Santa Cruz). Blots were incubated in primary antibody dilutions overnight at 4˚C, and then washed 3 times for 5 min in TBS/T. Blots were then incubated with the appropriate secondary antibody conjugated to HRP at 1:10,000 dilution for 1 hour at room temperature. After 3 more TBS/T washes, blots were developed and imaged.

Negative stain grid preparation

For random conical tilt experiments, I used C-flat holey carbon support grids (Protochips, prod #CF-2/.5-4C) that were coated with a thin layer of carbon evaporated onto mica and then floated on ultrapure water. For other negative stain experiments, I used standard carbon support grids (Ted Pella, G-400) coated with carbon by evaporation. All grids were glow discharged and then ~5 µL of sample was allowed to adsorb to the grid for approximately 20 seconds. Grids were then blotted dry and 2% uranyl formate was added for 2 minutes. After blotting excess uranyl formate and allowing to dry, grids were ready to image.

Random conical tilt data acquisition

Micrographs of untilted and -55˚ tilted views were acquired on a FEI T12 Spirit operated at 120 kV, spot size 5, 52000x nominal magnification, pixel size 2.07 Å, defocus values between -0.7 and -1.5 µm, and a dose of 30 $e^-/Å^2$. Data collection was automated using the MSI-RCT application within the Leginon software package (Suloway et al., 2005;Suloway et al., 2009). For 2-D analysis, data was collected using the MSI-Raster application.

EM data processing

Data was processed in the Appion pipeline with the following programs (Lander et al., 2009). Particles were picked using DoGPicker, and tilt-pairs were determined using AutoTiltPicker (Voss et al., 2009). The contrast transfer function was determined using CTFFind (Mindell and Grigorieff, 2003), and corrected using the EMAN 1.9 phase flip method. Individual particles were clustered using Xmipp 3 cl2d reference-free alignment to yield initial sets (Sorzano et al., 2010). After discarding classes with junk particles for several iterations, references were selected and used for reference-based alignment with the SPIDER AP MQ command (Frank et al., 1996). These references were then used to create RCT volumes using SPIDER within the Appion interface.

Protein crosslinking, sample preparation, and mass spectrometry.

Eluted proteins in 1 mL of 20 mM HEPES pH 8.5, 200 mM NaCl, and either 2 mM $CaCl_2$ or 2 mM EDTA were crosslinked with 10 mM Biotin-Aspartate Proline-PIR n-hydroxyphthalimide (BDP-NHP) (Weisbrod et al., 2013). As necessary, the pH was adjusted to ~8.0 with 100 µl of 200 mM HEPES pH 8.5. The reaction was allowed to continue for 1 hour at room temperature. Crosslinked proteins were denatured by the addition of urea buffer (8 M urea, 100 mM Tris-Cl pH 8.0), reduced (5 mM dithiothreitol, 30 min, 55˚C), and alkylated (15 mM iodoacetamide, 1 hour, dark, room temperature). Crosslinked proteins were then digested with sequencing grade trypsin (Promega) overnight at 37˚C. Resulting peptides were desalted with C18-SepPaks (Waters) and dried by vacuum centrifugation. Crosslinked peptides were injected onto an in-house pulled C8 column (3 µm, 200Å, Magic) and analyzed by Real-time analysis of crosslinked peptide technology (ReACT) (Weisbrod et al., 2013). Spectra generated from ReACT were searched against a target-decoy database using SEQUEST (Eng et al., 1994), as previously described (Weisbrod et al., 2013). Crosslinked sites were mapped to proteins using xiNet (Combe et al., 2015).

Structural modeling – Pymol/Chimera

Crosslinked peptides on PP2B, the PP2B/cyclosporine complex, and the PP2B/A238L complex were modeled using Pymol (Schrödinger). RCT volume data was modeled using Chimera (UCSF), and crystal structures were fit in the maps using the Fit in Map command.

GST protein-protein interaction assays

GST protein-protein interaction assays were performed as described previously (Gold et al., 2011). An LxVP peptide derived from NFATc1, or a scrambled version of this peptide, was added to a final concentration of 200 µM during the incubation step. The scrambled control version of this peptide was obtained by

writing each amino acid residue letter code onto a piece of paper, putting the pieces of paper into a hat, and asking a postdoc (Dr. Simon Amadeus Hinke) to draw one letter out at a time, with the order corresponding to the peptide sequence from the N-terminus to C-terminus. After the final wash, PP2B activity buffer (Calbiochem) was added and a phosphopeptide substrate was included to measure phosphatase activity in these samples.

Alphascreen competition assays

Alphascreen competition assays were performed in 25 mM HEPES, pH 7.5, 100 mM NaCl, 0.1% BSA, 3 mM $CaCl_2$, 2 µg/mL CaM. 10 µL of biotinylated PP2B and 10 µL of a His-tagged AKAP79 fragment (final concentration of each - 100 nM) were mixed and incubated for 15 minutes. 10 µL serial dilutions of untagged PP2B were added to the wells for 15 minutes and then Alphascreen beads (streptavidin donor, and nickel acceptor) were added and incubated for 60 minutes. Following this, the AlphaScreen signal was detected using a BMG PolarStar Omega plate reader. Data was analyzed using Prism 6.0 (GraphPad), and fit using a one-site IC50 model. Because of the concentrations used, the IC50 is able to approximate the Kd value of the interaction.

Solid phase peptide synthesis and overlay

Peptides were synthesized onto a cellulose membrane using the Intavis MultiPep solid-phase peptide synthesizer as described previously (Alto et al., 2003). 20-mers that stepped by 3 residues along the entire sequence of AKAP79 were spotted. After resolubilizing in ethanol, the peptides were overlaid with Flag-PP2B at ~1 mg/mL in 1% BSA/TBS-T in the presence of either 100 µg/mL CaM and 5 mM $CaCl_2$ or 5 mM EDTA. After washes in TBS/T supplemented with calcium or EDTA, the dot blots were developed.

Computational peptide/protein docking

The putative LxVP peptide in AKAP79 (KSRLKIPCIKFPRG) was computationally docked onto a crystallographic model of PP2B using the CABS-Dock server (Blaszczyk et al., 2015;Kurcinski et al., 2015). The peptide was assumed to form a random loop (as suggested by previous predictions), and the known binding site for the PxIxIT motif was excluded from being a possible binding site. The lowest energy conformation was assumed to be the most accurate binding prediction.

Design of AKAP79/CaNAR reporters

AKAP79 was fused to the N-terminal of the CaNAR2 sequence in the pcDNA 3.1 backbone. Mutation of the PxIxIT motif in NFAT (PRIEIT) to PRAEAT was done to abolish direct PP2B binding. Fusing a short peptide from AKAP79 to the CaNAR2 sequence and testing whether this was capable of producing a FRET response to ionomycin confirmed the sufficiency of the AKAP79 PxIxIT motif. After fusing the full-length sequence of AKAP79 to CaNAR, mutants were made which were lacking residues 122-136, 337-343, or both.

Confocal imaging of AKAP79-CaNAR mutants

HEK293 cells were seeded on 12 mm poly-D-lysine and laminin coated coverslips (Fisher cat#: 08-774-385) and transfected with 0.3 µg of the wild type and mutant CaNAR reporter constructs. After 48 hrs, cells were fixed in 4% paraformaldehyde at room temperature for 10 minutes and permeabilized for 1 hour in PBS with 0.1% Triton X-100. Coverslips were blocked in PBS with 10% donkey serum for 2 hours at room temperature before primary antibody staining overnight with mouse anti-PP2B antibody (BD Biosciences cat#: 610259). Samples were washed 3x and incubated with goat anti-mouse Alexafluor-555 secondary antibody. Nuclei were stained with DRAQ5 (Cell Signaling Technology, cat#: 4084) for 15 minutes at room temperature and then washed 3x before mounting in ProLong Gold anti-fade reagent (Invitrogen cat#: P36935) onto glass

microscope slides. Maximum projection images were acquired with a Zeiss scanning laser confocal microscope using a 63X oil immersion objective.

Immunoprecipitation of AKAP79-CaNAR

2 µg of each AKAP79-CaNAR variant were transfected into HEK293 cells for 48 hours. Cells were lysed in IP buffer (0.5% NP-40, 100 mM NaCl, 50 mM Tris-HCl, pH 7.4) supplemented with protease inhibitors. After lysates were cleared, they were incubated with 2 µg of mouse anti-GFP (Life Technologies), and 25 µL of protein A/G agarose for 2 hours. Following this, the beads were washed in IP buffer 3x and then SDS sample buffer was added. The samples were run on SDS-PAGE and transferred to nitrocellulose for western blotting as described above. 15 µg of lysate was also western blotted as an input.

FRET measurements in response to ionomycin, high and low levels

CaNAR2^{PAX} was generated by substituting the isoleucine residues at positions 115 and 117 within the NFAT domain of CaNAR2 (Mehta et al., 2014) with alanines (^{113}PRIEIT^{118} → ^{113}PRAEAT^{118}) via site-directed mutagenesis, thereby eliminating the endogenous calcineurin-docking PxIxIT motif. AKAP-tethered CaNAR2^{PAX} constructs were subsequently generated by PCR-amplifying full-length wild-type AKAP79, AKAP79$^{\Delta LKIP}$, AKAP79$^{\Delta PIX}$, and AKAP79$^{\Delta LKIP\Delta PIX}$ using *Hind*III/*Bam*HI-linker primers and ligating the resulting PCR fragments into *Hind*III/*Bam*HI-digested CaNAR2^{PAX} in pcDNA3, yielding AKAP79^{WT}-CaNAR2^{PAX}, AKAP79$^{\Delta LKIP}$-CaNAR2^{PAX}, AKAP79$^{\Delta PIX}$-CaNAR2^{PAX}, and AKAP79$^{\Delta LKIP\Delta PIX}$-CaNAR2^{PAX}, respectively. All constructs were verified by sequencing.

HeLa cells were cultured in Dulbecco minimal Eagle Medium (DMEM; Gibco, Grant Island, NY) containing 1 g/L D-glucose and supplemented with 10% fetal bovine serum (FBS; Sigma, St. Louis, MO) and 1% pen/strep (Sigma-Aldrich, St. Louis, MO). Cells were maintained at 37 °C in a humidified incubator with 5% CO_2. Prior to imaging experiments, cells were plated onto sterile 35-mm glass-

bottom dishes, transfected with the indicated biosensor constructs at 70-80% confluency using Lipofectamine2000 (Invitrogen), and then grown for and additional 48 h.

Cells were washed twice with Hank's Balanced Salt Solution (HBSS; Gibco) supplemented with 20 mM HEPES, pH 7.4, and 2.0 g/L D-glucose, then imaged in the dark at 37 °C. Ionomycin (iono; Calbiochem, San Diego, CA) was prepared at a stock concentration of 1 mM in DMSO and directly added to imaging dishes at the indicated concentrations. Images were acquired on an Zeiss Axio Observer.Z1 microscope (Carl Zeiss, Thornwood, NY) equipped with a 40x/1.3 NA oil-immersion objective lens, a Definite Focus system (Zeiss), and an electron-multiplying cooled charge-coupled device camera (Roper Scientific, Trenton, NJ) controlled by Metafluor 7.7 software (Molecular Devices, Sunnyvale, CA). Dual emission ratio imaging was performed using a 420DF20 excitation filter, a 450DRLP dichroic mirror, and two emission filters (475DF40 for CFP and 535DF25 for YFP). Filter sets were alternated using a Lambda 10-2 filter changer (Sutter Instruments, Novato, CA). Exposure times were 50–500 ms, and images were acquired every 30 s. Fluorescence was quantified in each channel by calculating the average fluorescence intensity in a manually defined region of interest (ROI). ROIs were draw around individual cells, and only cells with clear, plasma membrane-localized fluorescence were selected. Background correction of the fluorescence images was performed by subtracting the intensities of untransfected cells or regions of the imaging dish with no cells. Time-courses were normalized by setting the emission ratio before drug addition equal to one. Graphs were plotted using GraphPad Prism version 5.0f (GraphPad Software, La Jolla, CA), and statistical analyses were performed using the same software. Statistical significance was set at $p < 0.05$.

References

Akerboom, J., Carreras Calderon, N., Tian, L., Wabnig, S., Prigge, M., Tolo, J., Gordus, A., Orger, M.B., Severi, K.E., Macklin, J.J., Patel, R., Pulver, S.R., Wardill, T.J., Fischer, E., Schuler, C., Chen, T.W., Sarkisyan, K.S., Marvin, J.S., Bargmann, C.I., Kim, D.S., Kugler, S., Lagnado, L., Hegemann, P., Gottschalk, A., Schreiter, E.R., and Looger, L.L. (2013). Genetically encoded calcium indicators for multi-color neural activity imaging and combination with optogenetics. *Front Mol Neurosci* 6**,** 2. doi: 10.3389/fnmol.2013.00002.

Altier, C., Dubel, S.J., Barrere, C., Jarvis, S.E., Stotz, S.C., Spaetgens, R.L., Scott, J.D., Cornet, V., De Waard, M., Zamponi, G.W., Nargeot, J., and Bourinet, E. (2002). Trafficking of L-type calcium channels mediated by the postsynaptic scaffolding protein AKAP79. *J Biol Chem* 277**,** 33598-33603.

Alto, N.M., Soderling, S.H., Hoshi, N., Langeberg, L.K., Fayos, R., Jennings, P.A., and Scott, J.D. (2003). Bioinformatic design of A-kinase anchoring protein-in silico: A potent and selective peptide antagonist of type II protein kinase A anchoring. *Proc. Natl. Acad. Sci. U.S.A.* 100**,** 4445-4450.

Aramburu, J., Yaffe, M.B., Lopez-Rodriguez, C., Cantley, L.C., Hogan, P.G., and Rao, A. (1999). Affinity-driven peptide selection of an NFAT inhibitor more selective than cyclosporin A. *Science* 285**,** 2129-2133.

Baillie, G.S., Scott, J.D., and Houslay, M.D. (2005). Compartmentalisation of phosphodiesterases and protein kinase A: opposites attract. *FEBS Lett* 579**,** 3264-3270.

Barria, A., Derkach, V., and Soderling, T. (1997a). Identification of the Ca2+/calmodulin-dependent protein kinase II regulatory phosphorylation site in the alpha-amino-3-hydroxyl-5-methyl- 4-isoxazole-propionate-type glutamate receptor. *J Biol Chem* 272**,** 32727-32730.

Barria, A., Muller, D., Derkach, V., Griffith, L.C., and Soderling, T.R. (1997b). Regulatory phosphorylation of AMPA-type glutamate receptors by CaM-KII during long-term potentiation. *Science* 276**,** 2042-2045.

Behrmann, E., Loerke, J., Budkevich, T.V., Yamamoto, K., Schmidt, A., Penczek, P.A., Vos, M.R., Burger, J., Mielke, T., Scheerer, P., and Spahn, C.M. (2015). Structural snapshots of actively translating human ribosomes. *Cell* 161**,** 845-857. doi: 10.1016/j.cell.2015.03.052.

Blaszczyk, M., Kurcinski, M., Kouza, M., Wieteska, L., Debinski, A., Kolinski, A., and Kmiecik, S. (2015). Modeling of protein-peptide interactions using the CABS-dock web server for binding site search and flexible docking. *Methods*. doi: 10.1016/j.ymeth.2015.07.004.

Blumenthal, D.K., Takio, K., Hansen, R.S., and Krebs, E.G. (1986). Dephosphorylation of cAMP-dependent protein kinase regulatory subunit (type II) by calmodulin-dependent protein phosphatase. *J. Biol. Chem.* 261**,** 8140-8145.

Brandao, K.E., Dell'acqua, M.L., and Levinson, S.R. (2012). A-kinase anchoring protein 150 expression in a specific subset of TRPV1- and CaV 1.2-positive nociceptive rat dorsal root ganglion neurons. *J Comp Neurol* 520**,** 81-99. doi: 10.1002/cne.22692.

Burgers, P.P., Van Der Heyden, M.A., Kok, B., Heck, A.J., and Scholten, A. (2015). A systematic evaluation of protein kinase A-A-kinase anchoring protein interaction motifs. *Biochemistry* 54**,** 11-21. doi: 10.1021/bi500721a.

Burns-Hamuro, L.L., Hamuro, Y., Kim, J.S., Sigala, P., Fayos, R., Stranz, D.D., Jennings, P.A., Taylor, S.S., and Woods, V.L., Jr. (2005). Distinct interaction modes of an AKAP bound to two regulatory subunit isoforms of protein kinase A revealed by amide hydrogen/deuterium exchange. *Protein Sci* 14**,** 2982-2992. doi: 10.1110/ps.051687305.

Campbell, M.G., Cheng, A., Brilot, A.F., Moeller, A., Lyumkis, D., Veesler, D., Pan, J., Harrison, S.C., Potter, C.S., Carragher, B., and Grigorieff, N. (2012). Movies of ice-embedded particles enhance resolution in electron cryo-microscopy. *Structure* 20**,** 1823-1828. doi: 10.1016/j.str.2012.08.026.

Campbell, M.G., Kearney, B.M., Cheng, A., Potter, C.S., Johnson, J.E., Carragher, B., and Veesler, D. (2014). Near-atomic resolution reconstructions using a mid-range electron microscope operated at 200 kV. *J Struct Biol* 188**,** 183-187. doi: 10.1016/j.jsb.2014.09.008.

Campbell, M.G., Veesler, D., Cheng, A., Potter, C.S., and Carragher, B. (2015). 2.8 A resolution reconstruction of the Thermoplasma acidophilum 20S proteasome using cryo-electron microscopy. *Elife* 4. doi: 10.7554/eLife.06380.

Carlson, C.R., Lygren, B., Berge, T., Hoshi, N., Wong, W., Tasken, K., and Scott, J.D. (2006). Delineation of Type I Protein Kinase A-selective Signaling Events Using an RI Anchoring Disruptor. *J Biol Chem* 281**,** 21535-21545.

Carnegie, G.K., Means, C.K., and Scott, J.D. (2009). A-kinase anchoring proteins: from protein complexes to physiology and disease. *IUBMB Life* 61**,** 394-406. doi: 10.1002/iub.168.

Carr, D.W., Hausken, Z.E., Fraser, I.D., Stofko-Hahn, R.E., and Scott, J.D. (1992a). Association of the type II cAMP-dependent protein kinase with a human thyroid RII-anchoring protein. Cloning and characterization of the RII-binding domain. *J. Biol. Chem.* 267**,** 13376-13382.

Carr, D.W., Stofko-Hahn, R.E., Fraser, I.D., Bishop, S.M., Acott, T.S., Brennan, R.G., and Scott, J.D. (1991). Interaction of the regulatory subunit (RII) of cAMP-dependent protein kinase with RII-anchoring proteins occurs through an amphipathic helix binding motif. *J. Biol. Chem.* 266**,** 14188-14192.

Carr, D.W., Stofko-Hahn, R.E., Fraser, I.D.C., Cone, R.D., and Scott, J.D. (1992b). Localization of the cAMP-dependent protein kinase to the postsynaptic densities by A-kinase anchoring proteins: characterization of AKAP79. *J. Biol. Chem.* 24**,** 16816-16823.

Choy, M.S., Hieke, M., Kumar, G.S., Lewis, G.R., Gonzalez-Dewhitt, K.R., Kessler, R.P., Stein, B.J., Hessenberger, M., Nairn, A.C., Peti, W., and Page, R. (2014). Understanding the antagonism of retinoblastoma protein dephosphorylation by PNUTS provides insights into the PP1 regulatory code. *Proc Natl Acad Sci U S A* 111**,** 4097-4102. doi: 10.1073/pnas.1317395111.

Christian, F., Szaszak, M., Friedl, S., Drewianka, S., Lorenz, D., Goncalves, A., Furkert, J., Vargas, C., Schmieder, P., Gotz, F., Zuhlke, K., Moutty, M., Gottert, H., Joshi, M., Reif, B., Haase, H., Morano, I., Grossmann, S., Klukovits, A., Verli, J., Gaspar, R., Noack, C., Bergmann, M., Kass, R., Hampel, K., Kashin, D., Genieser, H.G., Herberg, F.W., Willoughby, D., Cooper, D.M., Baillie, G.S., Houslay, M.D., Von Kries, J.P., Zimmermann, B., Rosenthal, W., and Klussmann, E. (2011). Small molecule AKAP-protein kinase A (PKA) interaction disruptors that activate PKA interfere with compartmentalized cAMP signaling in cardiac myocytes. *J Biol Chem* 286**,** 9079-9096. doi: 10.1074/jbc.M110.160614.

Clipstone, N.A., and Crabtree, G.R. (1992). Identification of calcineurin as a key signalling enzyme in T-lymphocyte activation. *Nature* 357**,** 695-697.

Coghlan, V.M., Perrino, B.A., Howard, M., Langeberg, L.K., Hicks, J.B., Gallatin, W.M., and Scott, J.D. (1995). Association of protein kinase A and protein phosphatase 2B with a common anchoring protein. *Science* 267**,** 108-112.

Cohen, P., and Cohen, T.W. (1989). Protein phosphatases come of age. *J. Biol. Chem.* 264**,** 21435-21438.

Cohen, P.T. (2002). Protein phosphatase 1--targeted in many directions. *J. Cell Sci.* 115**,** 241-256.

Collas, P., Le Guellec, K., and Tasken, K. (1999). The A-kinase-anchoring protein AKAP95 is a multivalent protein with a key role in chromatin condensation at mitosis. *J Cell Biol* 147**,** 1167-1180.

Colledge, M., Dean, R.A., Scott, G.K., Langeberg, L.K., Huganir, R.L., and Scott, J.D. (2000). Targeting of PKA to glutamate receptors through a MAGUK-AKAP complex. *Neuron* 27**,** 107-119.

Combe, C.W., Fischer, L., and Rappsilber, J. (2015). xiNET: cross-link network maps with residue resolution. *Mol Cell Proteomics* 14**,** 1137-1147. doi: 10.1074/mcp.O114.042259.

Corbin, J.D., Keely, S.L., Soderling, T.R., and Park, C.R. (1975). Hormonal regulation of adenosine 3',5'-monophosphate-dependent protein kinase. *Adv Cyclic Nucleotide Res* 5**,** 265-279.

Corbin, J.D., Sugden, P.H., West, L., Flockhart, D.A., Lincoln, T.M., and Mccarthy, D. (1978). Studies on the properties and mode of action of the purified regulatory subunit of bovine heart adenosine 3':5'-monophosphate-dependent protein kinase. *J. Biol. Chem.* 253**,** 3997-4003.

Delint-Ramirez, I., Willoughby, D., Hammond, G.R., Ayling, L.J., and Cooper, D.M. (2011). Palmitoylation targets AKAP79 protein to lipid rafts and

promotes its regulation of calcium-sensitive adenylyl cyclase type 8. *J Biol Chem* 286**,** 32962-32975. doi: 10.1074/jbc.M111.243899.

Dell'acqua, M.L., Dodge, K.L., Tavalin, S.J., and Scott, J.D. (2002). Mapping the protein phosphatase-2B anchoring site on AKAP79. Binding and inhibition of phosphatase activity are mediated by residues 315-360. *J Biol Chem* 277**,** 48796-48802.

Dell'acqua, M.L., Faux, M.C., Thorburn, J., Thorburn, A., and Scott, J.D. (1998). Membrane-targeting sequences on AKAP79 bind phosphatidylinositol-4, 5- bisphosphate. *EMBO J.* 17**,** 2246-2260.

Dell'acqua, M.L., Smith, K.E., Gorski, J.A., Horne, E.A., Gibson, E.S., and Gomez, L.L. (2006). Regulation of neuronal PKA signaling through AKAP targeting dynamics. *Eur J Cell Biol* 85**,** 627-633.

Diller, T.C., Madhusudan, Xuong, N.H., and Taylor, S.S. (2001). Molecular basis for regulatory subunit diversity in cAMP-dependent protein kinase: crystal structure of the type II beta regulatory subunit. *Structure* 9**,** 73-82.

Diviani, D., Dodge-Kafka, K.L., Li, J., and Kapiloff, M.S. (2011). A-kinase anchoring proteins: scaffolding proteins in the heart. *Am J Physiol Heart Circ Physiol* 301**,** H1742-1753. doi: 10.1152/ajpheart.00569.2011.

Dosztanyi, Z., Csizmok, V., Tompa, P., and Simon, I. (2005a). IUPred: web server for the prediction of intrinsically unstructured regions of proteins based on estimated energy content. *Bioinformatics* 21**,** 3433-3434. doi: 10.1093/bioinformatics/bti541.

Dosztanyi, Z., Csizmok, V., Tompa, P., and Simon, I. (2005b). The pairwise energy content estimated from amino acid composition discriminates between folded and intrinsically unstructured proteins. *J Mol Biol* 347**,** 827-839. doi: 10.1016/j.jmb.2005.01.071.

Dosztanyi, Z., Meszaros, B., and Simon, I. (2009). ANCHOR: web server for predicting protein binding regions in disordered proteins. *Bioinformatics* 25**,** 2745-2746. doi: 10.1093/bioinformatics/btp518.

Efendiev, R., Samelson, B.K., Nguyen, B.T., Phatarpekar, P.V., Baameur, F., Scott, J.D., and Dessauer, C.W. (2010). AKAP79 interacts with multiple adenylyl cyclase (AC) isoforms and scaffolds AC5 and -6 to alpha-amino-3-hydroxyl-5-methyl-4-isoxazole-propionate (AMPA) receptors. *J Biol Chem* 285**,** 14450-14458. doi: M110.109769 [pii]
10.1074/jbc.M110.109769.

Eng, J.K., Mccormack, A.L., and Yates, J.R. (1994). An approach to correlate tandem mass spectral data of peptides with amino acid sequences in a protein database. *J Am Soc Mass Spectrom* 5**,** 976-989. doi: 10.1016/1044-0305(94)80016-2.

Escolano, A., Martinez-Martinez, S., Alfranca, A., Urso, K., Izquierdo, H.M., Delgado, M., Martin, F., Sabio, G., Sancho, D., Gomez-Del Arco, P., and Redondo, J.M. (2014). Specific calcineurin targeting in macrophages confers resistance to inflammation via MKP-1 and p38. *EMBO J* 33**,** 1117-1133. doi: 10.1002/embj.201386369.

Faux, M.C., and Scott, J.D. (1997). Regulation of the AKAP79-protein kinase C interaction by Ca2+/calmodulin. *J. Biol. Chem.* 272**,** 17038-17044.

Frank, J., Radermacher, M., Penczek, P., Zhu, J., Li, Y., Ladjadj, M., and Leith, A. (1996). SPIDER and WEB: processing and visualization of images in 3D electron microscopy and related fields. *J Struct Biol* 116**,** 190-199. doi: 10.1006/jsbi.1996.0030.

Gold, M.G., Fowler, D.M., Means, C.K., Pawson, C.T., Stephany, J.J., Langeberg, L.K., Fields, S., and Scott, J.D. (2013). Engineering A-kinase anchoring protein (AKAP)-selective regulatory subunits of protein kinase A (PKA) through structure-based phage selection. *J. Biol. Chem.* 288**,** 17111-17121. doi: 10.1074/jbc.M112.447326.

Gold, M.G., Lygren, B., Dokurno, P., Hoshi, N., Mcconnachie, G., Tasken, K., Carlson, C.R., Scott, J.D., and Barford, D. (2006). Molecular basis of AKAP specificity for PKA regulatory subunits. *Mol. Cell* 24**,** 383-395.

Gold, M.G., Reichow, S.L., O'neill, S.E., Weisbrod, C.R., Langeberg, L.K., Bruce, J.E., Gonen, T., and Scott, J.D. (2012). AKAP2 anchors PKA with aquaporin-0 to support ocular lens transparency. *EMBO molecular medicine* 4**,** 15-26. doi: 10.1002/emmm.201100184.

Gold, M.G., Smith, F.D., Scott, J.D., and Barford, D. (2008). AKAP18 contains a phosphoesterase domain that binds AMP. *Journal of molecular biology* 375**,** 1329-1343. doi: 10.1016/j.jmb.2007.11.037.

Gold, M.G., Stengel, F., Nygren, P.J., Weisbrod, C.R., Bruce, J.E., Robinson, C.V., Barford, D., and Scott, J.D. (2011). Architecture and dynamics of an A-kinase anchoring protein 79 (AKAP79) signaling complex. *Proc Natl Acad Sci U S A* 108**,** 6426-6431. doi: 10.1073/pnas.1014400108.

Gorski, J.A., Gomez, L.L., Scott, J.D., and Dell'acqua, M.L. (2005). Association of an A-kinase-anchoring protein signaling scaffold with cadherin adhesion molecules in neurons and epithelial cells. *Mol Biol Cell* 16**,** 3574-3590.

Grigoriu, S., Bond, R., Cossio, P., Chen, J.A., Ly, N., Hummer, G., Page, R., Cyert, M.S., and Peti, W. (2013). The molecular mechanism of substrate engagement and immunosuppressant inhibition of calcineurin. *PLoS Biol* 11**,** e1001492. doi: 10.1371/journal.pbio.1001492.

Hall, D.D., Davare, M.A., Shi, M., Allen, M.L., Weisenhaus, M., Mcknight, G.S., and Hell, J.W. (2007). Critical role of cAMP-dependent protein kinase anchoring to the L-type calcium channel Cav1.2 via A-kinase anchor protein 150 in neurons. *Biochemistry* 46**,** 1635-1646.

Helps, N.R., Brewis, N.D., Lineruth, K., Davis, T., Kaiser, K., and Cohen, P.T. (1998). Protein phosphatase 4 is an essential enzyme required for organisation of microtubules at centrosomes in Drosophila embryos. *J Cell Sci* 111**,** 1331-1340.

Hinke, S.A., Navedo, M.F., Ulman, A., Whiting, J.L., Nygren, P.J., Tian, G., Jimenez-Caliani, A.J., Langeberg, L.K., Cirulli, V., Tengholm, A., Dell'acqua, M.L., Santana, L.F., and Scott, J.D. (2012). Anchored

phosphatases modulate glucose homeostasis. *EMBO J.* 31**,** 3991-4004. doi: 10.1038/emboj.2012.244.

Hirsch, A.H., Glantz, S.B., Li, Y., You, Y., and Rubin, C.S. (1992). Cloning and expression of an intronless gene for AKAP75, an anchor protein for the regulatory subunit of cAMP-dependent protein kinase IIb. *J. Biol. Chem.* 267**,** 2131-2134.

Hoshi, N., Langeberg, L.K., and Scott, J.D. (2005). Distinct enzyme combinations in AKAP signalling complexes permit functional diversity. *Nat. Cell Biol.* 7**,** 1066-1073.

Hoshi, N., Zhang, J.S., Omaki, M., Takeuchi, T., Yokoyama, S., Wanaverbecq, N., Langeberg, L.K., Yoneda, Y., Scott, J.D., Brown, D.A., and Higashida, H. (2003). AKAP150 signaling complex promotes suppression of the M-current by muscarinic agonists. *Nat Neurosci* 6**,** 564-571. doi: 10.1038/nn1062.

Huang, L.J., Durick, K., Weiner, J.A., Chun, J., and Taylor, S.S. (1997a). D-AKAP2, a novel protein kinase A anchoring protein with a putative RGS domain. *Proc. Natl. Acad. Sci. USA* 94**,** 11184-11189.

Huang, L.J., Durick, K., Weiner, J.A., Chun, J., and Taylor, S.S. (1997b). Identification of a novel dual specificity protein kinase A anchoring protein, D-AKAP1. *J. Biol. Chem.* 272**,** 8057-8064.

Hubbard, M.J., Dent, P., Smythe, C., and Cohen, P. (1990). Targeting of protein phosphatase 1 to the sarcoplasmic reticulum of rabbit skeletal muscle by a protein that is very similar or identical to the G subunit that directs the enzyme to glycogen. *Eur. J. Biochem.* 189**,** 243-249.

Jurado, S., Biou, V., and Malenka, R.C. (2010). A calcineurin/AKAP complex is required for NMDA receptor-dependent long-term depression. *Nat Neurosci* 13**,** 1053-1055. doi: 10.1038/nn.2613.

Kang, S., Li, H., Rao, A., and Hogan, P.G. (2005). Inhibition of the calcineurin-NFAT interaction by small organic molecules reflects binding at an allosteric site. *J Biol Chem* 280**,** 37698-37706. doi: 10.1074/jbc.M502247200.

Kastner, B., Fischer, N., Golas, M.M., Sander, B., Dube, P., Boehringer, D., Hartmuth, K., Deckert, J., Hauer, F., Wolf, E., Uchtenhagen, H., Urlaub, H., Herzog, F., Peters, J.M., Poerschke, D., Luhrmann, R., and Stark, H. (2008). GraFix: sample preparation for single-particle electron cryomicroscopy. *Nat Methods* 5**,** 53-55. doi: 10.1038/nmeth1139.

Keith, D.J., Sanderson, J.L., Gibson, E.S., Woolfrey, K.M., Robertson, H.R., Olszewski, K., Kang, R., El-Husseini, A., and Dell'acqua, M.L. (2012). Palmitoylation of A-kinase anchoring protein 79/150 regulates dendritic endosomal targeting and synaptic plasticity mechanisms. *J Neurosci* 32**,** 7119-7136. doi: 10.1523/JNEUROSCI.0784-12.2012.

Kennedy, E.J., and Scott, J.D. (2015). Selective disruption of the AKAP signaling complexes. *Methods Mol Biol* 1294**,** 137-150. doi: 10.1007/978-1-4939-2537-7_11.

Kinderman, F.S., Kim, C., Von Daake, S., Ma, Y., Pham, B.Q., Spraggon, G., Xuong, N.H., Jennings, P.A., and Taylor, S.S. (2006). A dynamic mechanism for AKAP binding to RII isoforms of cAMP-dependent protein kinase. *Mol Cell* 24**,** 397-408.

Klauck, T.M., Faux, M.C., Labudda, K., Langeberg, L.K., Jaken, S., and Scott, J.D. (1996). Coordination of three signaling enzymes by AKAP79, a mammalian scaffold protein. *Science* 271**,** 1589-1592.

Kovanich, D., Van Der Heyden, M.A., Aye, T.T., Van Veen, T.A., Heck, A.J., and Scholten, A. (2010). Sphingosine kinase interacting protein is an A-kinase anchoring protein specific for type I cAMP-dependent protein kinase. *Chembiochem* 11**,** 963-971. doi: 10.1002/cbic.201000058.

Kurcinski, M., Jamroz, M., Blaszczyk, M., Kolinski, A., and Kmiecik, S. (2015). CABS-dock web server for the flexible docking of peptides to proteins without prior knowledge of the binding site. *Nucleic Acids Res* 43**,** W419-424. doi: 10.1093/nar/gkv456.

Lacana, E., Maceyka, M., Milstien, S., and Spiegel, S. (2002). Cloning and characterization of a protein kinase A anchoring protein (AKAP)-related protein that interacts with and regulates sphingosine kinase 1 activity. *J Biol Chem* 277**,** 32947-32953. doi: 10.1074/jbc.M202841200

M202841200 [pii].

Lander, G.C., Stagg, S.M., Voss, N.R., Cheng, A., Fellmann, D., Pulokas, J., Yoshioka, C., Irving, C., Mulder, A., Lau, P.W., Lyumkis, D., Potter, C.S., and Carragher, B. (2009). Appion: an integrated, database-driven pipeline to facilitate EM image processing. *J Struct Biol* 166**,** 95-102.

Langeberg, L.K., and Scott, J.D. (2015). Signalling scaffolds and local organization of cellular behaviour. *Nat Rev Mol Cell Biol* 16**,** 232-244. doi: 10.1038/nrm3966.

Li, H., Pink, M.D., Murphy, J.G., Stein, A., Dell'acqua, M.L., and Hogan, P.G. (2012). Balanced interactions of calcineurin with AKAP79 regulate Ca(2+)-calcineurin-NFAT signaling. *Nat. Struct. Mol. Biol.* 19**,** 337-345. doi: 10.1038/nsmb.2238.

Li, H., Rao, A., and Hogan, P.G. (2011). Interaction of calcineurin with substrates and targeting proteins. *Trends Cell Biol* 21**,** 91-103. doi: 10.1016/j.tcb.2010.09.011.

Li, H., Zhang, L., Rao, A., Harrison, S.C., and Hogan, P.G. (2007). Structure of calcineurin in complex with PVIVIT peptide: portrait of a low-affinity signalling interaction. *J Mol Biol* 369**,** 1296-1306. doi: 10.1016/j.jmb.2007.04.032.

Li, J., Negro, A., Lopez, J., Bauman, A.L., Henson, E., Dodge-Kafka, K., and Kapiloff, M.S. (2010). The mAKAPbeta scaffold regulates cardiac myocyte hypertrophy via recruitment of activated calcineurin. *J Mol Cell Cardiol* 48**,** 387-394. doi: 10.1016/j.yjmcc.2009.10.023.

Li, X., Romero, P., Rani, M., Dunker, A.K., and Obradovic, Z. (1999). Predicting Protein Disorder for N-, C-, and Internal Regions. *Genome Inform Ser Workshop Genome Inform* 10**,** 30-40.

Lin, J.W., Wyszynski, M., Madhavan, R., Sealock, R., Kim, J.U., and Sheng, M. (1998). Yotiao, a novel protein of neuromuscular junction and brain that interacts with specific splice variants of NMDA receptor subunit NR1. *J. Neurosci.* 18**,** 2017-2027.

Liu, J., Farmer, J.D.J., Lane, W.L., Friedman, J., Weissman, I., and Schreiber, S.L. (1991). Calcineurin is a common target of cyclophilin-cyclosporin A and FKBP-FK506 complexes. *Cell* 66**,** 807-815.

Lu, Y., Allen, M., Halt, A.R., Weisenhaus, M., Dallapiazza, R.F., Hall, D.D., Usachev, Y.M., Mcknight, G.S., and Hell, J.W. (2007). Age-dependent requirement of AKAP150-anchored PKA and GluR2-lacking AMPA receptors in LTP. *Embo J* 26**,** 4879-4890.

Malinow, R., and Malenka, R.C. (2002). AMPA receptor trafficking and synaptic plasticity. *Annu Rev Neurosci* 25**,** 103-126.

Matsoukas, M.T., Aranguren-Ibanez, A., Lozano, T., Nunes, V., Lasarte, J.J., Pardo, L., and Perez-Riba, M. (2015). Identification of small-molecule inhibitors of calcineurin-NFATc signaling that mimic the PxIxIT motif of calcineurin binding partners. *Sci Signal* 8**,** ra63. doi: 10.1126/scisignal.2005918.

Means, C.K., Lygren, B., Langeberg, L.K., Jain, A., Dixon, R.E., Vega, A.L., Gold, M.G., Petrosyan, S., Taylor, S.S., Murphy, A.N., Ha, T., Santana, L.F., Tasken, K., and Scott, J.D. (2011). An entirely specific type I A-kinase anchoring protein that can sequester two molecules of protein kinase A at mitochondria. *Proc. Natl. Acad. Sci. U. S. A.* 108**,** E1227-1235. doi: 10.1073/pnas.1107182108.

Mehta, S., Aye-Han, N.N., Ganesan, A., Oldach, L., Gorshkov, K., and Zhang, J. (2014). Calmodulin-controlled spatial decoding of oscillatory Ca2+ signals by calcineurin. *Elife* 3**,** e03765. doi: 10.7554/eLife.03765.

Mehta, S., Li, H., Hogan, P.G., and Cunningham, K.W. (2009). Domain architecture of the regulators of calcineurin (RCANs) and identification of a divergent RCAN in yeast. *Mol Cell Biol* 29**,** 2777-2793. doi: 10.1128/MCB.01197-08.

Mehta, S., and Zhang, J. (2014). Using a genetically encoded FRET-based reporter to visualize calcineurin phosphatase activity in living cells. *Methods Mol Biol* 1071**,** 139-149. doi: 10.1007/978-1-62703-622-1_11.

Meszaros, B., Simon, I., and Dosztanyi, Z. (2009). Prediction of protein binding regions in disordered proteins. *PLoS Comput Biol* 5**,** e1000376. doi: 10.1371/journal.pcbi.1000376.

Mindell, J.A., and Grigorieff, N. (2003). Accurate determination of local defocus and specimen tilt in electron microscopy. *Journal of structural biology* 142**,** 334-347.

Mooney, C., Pollastri, G., Shields, D.C., and Haslam, N.J. (2012). Prediction of short linear protein binding regions. *J Mol Biol* 415**,** 193-204. doi: 10.1016/j.jmb.2011.10.025.

Moorhead, G.B., Trinkle-Mulcahy, L., and Ulke-Lemee, A. (2007). Emerging roles of nuclear protein phosphatases. *Nat Rev Mol Cell Biol* 8**,** 234-244. doi: 10.1038/nrm2126.

Morishita, W., Connor, J.H., Xia, H., Quinlan, E.M., Shenolikar, S., and Malenka, R.C. (2001). Regulation of synaptic strength by protein phosphatase 1. *Neuron* 32**,** 1133-1148.

Mulkey, R.M., Endo, S., Shenolikar, S., and Malenka, R.C. (1994). Involvement of a calcineurin/inhibitor-1 phosphatase cascade in hippocampal long-term depression. *Nature* 369**,** 486-488.

Newlon, M.G., Roy, M., Morikis, D., Carr, D.W., Westphal, R., Scott, J.D., and Jennings, P.A. (2001). A novel mechanism of PKA anchoring revealed by solution structures of anchoring complexes. *Embo J* 20**,** 1651-1662.

Newlon, M.G., Roy, M., Morikis, D., Hausken, Z.E., Coghlan, V., Scott, J.D., and Jennings, P.A. (1999). The molecular basis for protein kinase A anchoring revealed by solution NMR. *Nat. Struct. Biol.* 6**,** 222-227.

Nystoriak, M.A., Nieves-Cintron, M., Nygren, P.J., Hinke, S.A., Nichols, C.B., Chen, C.Y., Puglisi, J.L., Izu, L.T., Bers, D.M., Dell'acqua, M.L., Scott, J.D., Santana, L.F., and Navedo, M.F. (2014). AKAP150 Contributes to Enhanced Vascular Tone by Facilitating Large-Conductance Ca2+-Activated K+ Channel Remodeling in Hyperglycemia and Diabetes Mellitus. *Circ Res* 114**,** 607-615. doi: 10.1161/CIRCRESAHA.114.302168.

Oliveria, S.F., Dell'acqua, M.L., and Sather, W.A. (2007). AKAP79/150 anchoring of calcineurin controls neuronal L-type Ca2+ channel activity and nuclear signaling. *Neuron* 55**,** 261-275.

Peng, M., Aye, T.T., Snel, B., Van Breukelen, B., Scholten, A., and Heck, A.J. (2015). Spatial Organization in Protein Kinase A Signaling Emerged at the Base of Animal Evolution. *J Proteome Res* 14**,** 2976-2987. doi: 10.1021/acs.jproteome.5b00370.

Reed, B.J., Locke, M.N., and Gardner, R.G. (2015). A Conserved Deubiquitinating Enzyme Uses Intrinsically Disordered Regions to Scaffold Multiple Protein-Interaction Sites. *J Biol Chem*. doi: 10.1074/jbc.M115.650952.

Reiterer, V., Eyers, P.A., and Farhan, H. (2014). Day of the dead: pseudokinases and pseudophosphatases in physiology and disease. *Trends Cell Biol.* doi: 10.1016/j.tcb.2014.03.008.

Ren, S., Uversky, V.N., Chen, Z., Dunker, A.K., and Obradovic, Z. (2008). Short Linear Motifs recognized by SH2, SH3 and Ser/Thr Kinase domains are conserved in disordered protein regions. *BMC Genomics* 9 Suppl 2**,** S26. doi: 10.1186/1471-2164-9-S2-S26.

Rodriguez, A., Roy, J., Martinez-Martinez, S., Lopez-Maderuelo, M.D., Nino-Moreno, P., Orti, L., Pantoja-Uceda, D., Pineda-Lucena, A., Cyert, M.S.,

and Redondo, J.M. (2009). A conserved docking surface on calcineurin mediates interaction with substrates and immunosuppressants. *Mol Cell* 33**,** 616-626. doi: 10.1016/j.molcel.2009.01.030.

Roy, J., and Cyert, M.S. (2009). Cracking the phosphatase code: docking interactions determine substrate specificity. *Sci Signal* 2**,** re9. doi: 10.1126/scisignal.2100re9.

Roy, J., Li, H., Hogan, P.G., and Cyert, M.S. (2007). A conserved docking site modulates substrate affinity for calcineurin, signaling output, and in vivo function. *Mol Cell* 25**,** 889-901. doi: 10.1016/j.molcel.2007.02.014.

Sanderson, J.L., and Dell'acqua, M.L. (2011). AKAP signaling complexes in regulation of excitatory synaptic plasticity. *Neuroscientist* 17**,** 321-336. doi: 10.1177/1073858410384740.

Sanderson, J.L., Gorski, J.A., Gibson, E.S., Lam, P., Freund, R.K., Chick, W.S., and Dell'acqua, M.L. (2012). AKAP150-anchored calcineurin regulates synaptic plasticity by limiting synaptic incorporation of Ca2+-permeable AMPA receptors. *J. Neurosci.* 32**,** 15036-15052. doi: 10.1523/JNEUROSCI.3326-12.2012.

Sarkar, D., Erlichman, J., and Rubin, C.S. (1984). Identification of a calmodulin-binding protein that co-purifies with the regulatory subunit of brain protein kinase II. *J. Biol. Chem.* 259**,** 9840-9846.

Sarma, G.N., Kinderman, F.S., Kim, C., Von Daake, S., Chen, L., Wang, B.C., and Taylor, S.S. (2010). Structure of D-AKAP2:PKA RI complex: insights into AKAP specificity and selectivity. *Structure* 18**,** 155-166. doi: S0969-2126(10)00007-9 [pii]

10.1016/j.str.2009.12.012.

Schachterle, C., Christian, F., Fernandes, J.M., and Klussmann, E. (2015). Screening for small molecule disruptors of AKAP-PKA interactions. *Methods Mol Biol* 1294**,** 151-166. doi: 10.1007/978-1-4939-2537-7_12.

Schafer, G., Milic, J., Eldahshan, A., Gotz, F., Zuhlke, K., Schillinger, C., Kreuchwig, A., Elkins, J.M., Abdul Azeez, K.R., Oder, A., Moutty, M.C., Masada, N., Beerbaum, M., Schlegel, B., Niquet, S., Schmieder, P., Krause, G., Von Kries, J.P., Cooper, D.M., Knapp, S., Rademann, J., Rosenthal, W., and Klussmann, E. (2013). Highly functionalized terpyridines as competitive inhibitors of AKAP-PKA interactions. *Angew Chem Int Ed Engl* 52**,** 12187-12191. doi: 10.1002/anie.201304686.

Schillace, R.V., and Scott, J.D. (1999). Association of the type 1 protein phosphatase PP1 with the A-kinase anchoring protein AKAP220. *Curr. Biol.* 9**,** 321-324. doi: S0960-9822(99)80141-9 [pii].

Schillace, R.V., Voltz, J.W., Sim, A.T., Shenolikar, S., and Scott, J.D. (2001). Multiple interactions within the AKAP220 signaling complex contribute to protein phosphatase 1 regulation. *J Biol Chem* 276**,** 12128-12134. doi: 10.1074/jbc.M010398200 [doi]

M010398200 [pii].

Schnizler, K., Shutov, L.P., Van Kanegan, M.J., Merrill, M.A., Nichols, B., Mcknight, G.S., Strack, S., Hell, J.W., and Usachev, Y.M. (2008). Protein kinase A anchoring via AKAP150 is essential for TRPV1 modulation by forskolin and prostaglandin E2 in mouse sensory neurons. *J Neurosci* 28**,** 4904-4917. doi: 10.1523/JNEUROSCI.0233-08.2008.

Scott, J.D., Stofko, R.E., Mcdonald, J.R., Comer, J.D., Vitalis, E.A., and Mangeli, J. (1990). Type II regulatory subunit dimerization determines the subcellular localization of the cAMP-dependent protein kinase. *J. Biol. Chem.* 265**,** 21561-21566.

Shih, M., Lin, F., Scott, J.D., Wang, H.Y., and Malbon, C.C. (1999). Dynamic complexes of beta2-adrenergic receptors with protein kinases and phosphatases and the role of gravin. *J. Biol. Chem.* 274**,** 1588-1595.

Singh, A., Redden, J.M., Kapiloff, M.S., and Dodge-Kafka, K.L. (2011). The large isoforms of A-kinase anchoring protein 18 mediate the phosphorylation of inhibitor-1 by protein kinase A and the inhibition of protein phosphatase 1 activity. *Mol Pharmacol* 79**,** 533-540. doi: 10.1124/mol.110.065425.

Singh, M., Singh, P., Vaira, D., Torheim, E.A., Rahmouni, S., Tasken, K., and Moutschen, M. (2014). The RIAD peptidomimetic inhibits HIV-1 replication in humanized NSG mice. *Eur J Clin Invest* 44**,** 146-152. doi: 10.1111/eci.12200.

Smith, F.D., Reichow, S.L., Esseltine, J.L., Shi, D., Langeberg, L.K., Scott, J.D., and Gonen, T. (2013). Intrinsic disorder within an AKAP-protein kinase A complex guides local substrate phosphorylation. *Elife* 2**,** e01319. doi: 10.7554/eLife.01319.

Sorzano, C.O., Bilbao-Castro, J.R., Shkolnisky, Y., Alcorlo, M., Melero, R., Caffarena-Fernandez, G., Li, M., Xu, G., Marabini, R., and Carazo, J.M. (2010). A clustering approach to multireference alignment of single-particle projections in electron microscopy. *J Struct Biol* 171**,** 197-206. doi: 10.1016/j.jsb.2010.03.011.

Stark, H. (2010). GraFix: stabilization of fragile macromolecular complexes for single particle cryo-EM. *Methods Enzymol* 481**,** 109-126. doi: 10.1016/S0076-6879(10)81005-5.

Steen, R.L., Martins, S.B., Tasken, K., and Collas, P. (2000). Recruitment of protein phosphatase 1 to the nuclear envelope by A- kinase anchoring protein AKAP149 is a prerequisite for nuclear lamina assembly . *J. Cell Biol.* 150**,** 1251-1262.

Stefan, E., Wiesner, B., Baillie, G.S., Mollajew, R., Henn, V., Lorenz, D., Furkert, J., Santamaria, K., Nedvetsky, P., Hundsrucker, C., Beyermann, M., Krause, E., Pohl, P., Gall, I., Macintyre, A.N., Bachmann, S., Houslay, M.D., Rosenthal, W., and Klussmann, E. (2007). Compartmentalization of cAMP-dependent signaling by phosphodiesterase-4D is involved in the regulation of vasopressin-mediated water reabsorption in renal principal cells. *J Am Soc Nephrol* 18**,** 199-212. doi: ASN.2006020132 [pii]
10.1681/ASN.2006020132.

Stewart, A.A., Ingebritsen, T.S., Manalan, A., Klee, C.B., and Cohen, P. (1982). Discovery of a Ca2+- and calmodulin-dependent protein phosphatase: probable identity with calcineurin (CaM-BP80). *FEBS Lett* 137**,** 80-84.

Stralfors, P., Hiraga, A., and Cohen, P. (1985). The protein phosphatases involved in cellular regulation. Purification and characterisation of the glycogen-bound form of protein phosphatase- 1 from rabbit skeletal muscle. *Eur J Biochem* 149**,** 295-303.

Su, Y., Dostmann, W.R.G., Herberg, F.W., Durick, K., Xuong, N.-H., Ten Eyck, L., Taylor, S.S., and Varughese, K.I. (1995). Regulatory subunit of protein kinase A: structure of deletion mutant with cAMP binding proteins. *Science* 269**,** 807-813.

Suloway, C., Pulokas, J., Fellmann, D., Cheng, A., Guerra, F., Quispe, J., Stagg, S., Potter, C.S., and Carragher, B. (2005). Automated molecular microscopy: the new Leginon system. *J Struct Biol* 151**,** 41-60. doi: 10.1016/j.jsb.2005.03.010.

Suloway, C., Shi, J., Cheng, A., Pulokas, J., Carragher, B., Potter, C.S., Zheng, S.Q., Agard, D.A., and Jensen, G.J. (2009). Fully automated, sequential tilt-series acquisition with Leginon. *J Struct Biol* 167**,** 11-18. doi: 10.1016/j.jsb.2009.03.019.

Tandan, S., Wang, Y., Wang, T.T., Jiang, N., Hall, D.D., Hell, J.W., Luo, X., Rothermel, B.A., and Hill, J.A. (2009). Physical and functional interaction between calcineurin and the cardiac L-type Ca2+ channel. *Circ Res* 105**,** 51-60. doi: CIRCRESAHA.109.199828 [pii]
10.1161/CIRCRESAHA.109.199828.

Tanji, C., Yamamoto, H., Yorioka, N., Kohno, N., Kikuchi, K., and Kikuchi, A. (2002). A-kinase anchoring protein AKAP220 binds to glycogen synthase kinase-3beta (GSK-3beta) and mediates protein kinase A-dependent inhibition of GSK-3beta. *J. Biol. Chem.* 277**,** 36955-36961.

Taylor, S.S., Ilouz, R., Zhang, P., and Kornev, A.P. (2012). Assembly of allosteric macromolecular switches: lessons from PKA. *Nat Rev Mol Cell Biol* 13**,** 646-658. doi: 10.1038/nrm3432.

Theurkauf, W.E., and Vallee, R.B. (1982). Molecular characterization of the cAMP-dependent protein kinase bound to microtubule-associated protein 2. *J. Biol. Chem.* 257**,** 3284-3290.

Troger, J., Moutty, M.C., Skroblin, P., and Klussmann, E. (2012). A-kinase anchoring proteins as potential drug targets. *Br J Pharmacol* 166**,** 420-433. doi: 10.1111/j.1476-5381.2011.01796.x.

Van Roey, K., Uyar, B., Weatheritt, R.J., Dinkel, H., Seiler, M., Budd, A., Gibson, T.J., and Davey, N.E. (2014). Short linear motifs: ubiquitous and functionally diverse protein interaction modules directing cell regulation. *Chem Rev* 114**,** 6733-6778. doi: 10.1021/cr400585q.

Veesler, D., Cupelli, K., Burger, M., Graber, P., Stehle, T., and Johnson, J.E. (2014). Single-particle EM reveals plasticity of interactions between the

adenovirus penton base and integrin alphaVbeta3. *Proc Natl Acad Sci U S A* 111**,** 8815-8819. doi: 10.1073/pnas.1404575111.

Vigil, D., Blumenthal, D.K., Heller, W.T., Brown, S., Canaves, J.M., Taylor, S.S., and Trewhella, J. (2004). Conformational differences among solution structures of the type Ialpha, IIalpha and IIbeta protein kinase A regulatory subunit homodimers: role of the linker regions. *J Mol Biol* 337**,** 1183-1194. doi: 10.1016/j.jmb.2004.02.028.

Vijayaraghavan, S., Goueli, S.A., Davey, M.P., and Carr, D.W. (1997). Protein kinase A-anchoring inhibitor peptides arrest mammalian sperm motility. *J. Biol. Chem.* 272**,** 4747-4752.

Viswanatha, R., Wayt, J., Ohouo, P.Y., Smolka, M.B., and Bretscher, A. (2013). Interactome analysis reveals ezrin can adopt multiple conformational states. *J Biol Chem* 288**,** 35437-35451. doi: 10.1074/jbc.M113.505669.

Voss, N.R., Yoshioka, C.K., Radermacher, M., Potter, C.S., and Carragher, B. (2009). DoG Picker and TiltPicker: software tools to facilitate particle selection in single particle electron microscopy. *J Struct Biol* 166**,** 205-213.

Walsh, D.A., Perkins, J.P., and Krebs, E.G. (1968). An adenosine 3',5'-monophosphate-dependent protein kinase from rabbit skeletal muscle. *J. Biol. Chem.* 243**,** 3763-3765.

Wang, Y., Ho, T.G., Bertinetti, D., Neddermann, M., Franz, E., Mo, G.C., Schendowich, L.P., Sukhu, A., Spelts, R.C., Zhang, J., Herberg, F.W., and Kennedy, E.J. (2014). Isoform-selective disruption of AKAP-localized PKA using hydrocarbon stapled peptides. *ACS Chem Biol* 9**,** 635-642. doi: 10.1021/cb400900r.

Wang, Y., Ho, T.G., Franz, E., Hermann, J.S., Smith, F.D., Hehnly, H., Esseltine, J.L., Hanold, L.E., Murph, M.M., Bertinetti, D., Scott, J.D., Herberg, F.W., and Kennedy, E.J. (2015). PKA-Type I Selective Constrained Peptide Disruptors of AKAP Complexes. *ACS Chem Biol* 10**,** 1502-1510. doi: 10.1021/acschembio.5b00009.

Weisbrod, C.R., Chavez, J.D., Eng, J.K., Yang, L., Zheng, C., and Bruce, J.E. (2013). In vivo protein interaction network identified with a novel real-time cross-linked peptide identification strategy. *J Proteome Res* 12**,** 1569-1579. doi: 10.1021/pr3011638.

Welch, E.J., Jones, B.W., and Scott, J.D. (2010). Networking with AKAPs: context-dependent regulation of anchored enzymes. *Mol. Interv.* 10**,** 86-97.

Westphal, R.S., Tavalin, S.J., Lin, J.W., Alto, N.M., Fraser, I.D., Langeberg, L.K., Sheng, M., and Scott, J.D. (1999). Regulation of NMDA receptors by an associated phosphatase-kinase signaling complex. *Science* 285**,** 93-96.

Williams, K.R., Hemmings, H.C., Jr., Lopresti, M.B., Konigsberg, W.H., and Greengard, P. (1986). DARPP-32, a dopamine- and cyclic AMP-regulated neuronal phosphoprotein. Primary structure and homology with protein phosphatase inhibitor-1. *J Biol Chem* 261**,** 1890-1903.

Willoughby, D., Masada, N., Wachten, S., Pagano, M., Halls, M.L., Everett, K.L., Ciruela, A., and Cooper, D.M. (2010). AKAP79/150 interacts with AC8 and

regulates Ca2+-dependent cAMP synthesis in pancreatic and neuronal systems. *J Biol Chem* 285**,** 20328-20342. doi: M110.120725 [pii] 10.1074/jbc.M110.120725.

Wong, W., and Scott, J.D. (2004). AKAP Signalling complexes: Focal points in space and time. *Nature Rev. Mol. Cell Biol.* 5**,** 959-971.

Wu, J., Brown, S.H., Von Daake, S., and Taylor, S.S. (2007). PKA type IIalpha holoenzyme reveals a combinatorial strategy for isoform diversity. *Science* 318**,** 274-279. doi: 10.1126/science.1146447.

Zawadzki, K.M., and Taylor, S.S. (2004). cAMP-dependent protein kinase regulatory subunit type IIbeta: active site mutations define an isoform-specific network for allosteric signaling by cAMP. *J Biol Chem* 279**,** 7029-7036. doi: 10.1074/jbc.M310804200.

Zhang, P., Smith-Nguyen, E.V., Keshwani, M.M., Deal, M.S., Kornev, A.P., and Taylor, S.S. (2012). Structure and allostery of the PKA RIIbeta tetrameric holoenzyme. *Science* 335**,** 712-716. doi: 10.1126/science.1213979.